Original Article

Development and validation of the prognostic value of the immune-related genes in clear cell renal cell carcinoma

Zhuangyao Liao, Haohua Yao, Jinhuan Wei, Zihao Feng, Wei Chen, Junhang Luo, Xu Chen

Department of Urology, The First Affiliated Hospital of Sun Yat-Sen University, Guangzhou, China

Contributions: (I) Conception and design: Z Liao; (II) Administrative support: X Chen, W Chen, J Luo; (III) Provision of study materials: H Yao; (IV) Collection and assembly of data: J Wei; (V) Data analysis: Z Liao, Z Feng; (VI) Manuscript writing: Z Liao, X Chen; (VII) Final approval of manuscript: All authors.

Correspondence to: Xu Chen. Department of Urology, The First Affiliated Hospital, Sun Yat-Sen University, Guangzhou 510080, China.
Email: chenxu25@mail.sysu.edu.cn.

Background: Clear cell renal cell carcinoma (ccRCC) is a highly heterogeneous tumor, resulting a challenge of developing target therapeutics. Not long ago, immune checkpoint blockade regimens combine with tyrosin kinase inhibitors have evolved frontline options in metastatic RCC, which implies arrival of the era of tumor immunotherapy. Studies have demonstrated immune-related genes (IRGs) could characterize tumor milieu and related to patient survival. Nevertheless, the clinical significance of classifier depending on IRGs in ccRCC has not been well established.

Methods: The R package limma, univariate and LASSO cox regression analysis were used to screen the prognostic related IRGs from TCGA database. Multivariate cox regression was utilized to establish a risk prediction model for candidate genes. Quantitative real-time PCR was used to confirm the expression of candidates in clinical samples from our institution. CIBERSORT algorithm and correlation analysis were applied to explore tumor-infiltrating immune cells signature between different risk groups. A clinical nomogram was also developed to predict OS by using the rms R package based on the risk prediction model and other independent risk factors. The ICGC data was used for external validation of either gene risk model or nomogram.

Results: We identified 382 differentially expressed immune related genes. Four unique prognostic IRGs (CRABP2, LTB4R, PTGER1 and TEK) were finally affirmed to associate with tumor survival independently and utilized to establish the risk score model. All candidates' expression was successfully laboratory confirmed by q-PCR. CIBERSORT analysis implied patients in unfavorable-risk group with high CD8 T cell, regulatory T cell and NK cell infiltration, as well as high expression of PD-1, CTLA4, TNFRSF9, TIGIT and LAG3. A nomogram combined IRGs risk score with age, gender, TNM stage, Fuhrman grade, necrosis was further generated to predict of 3- and 5-year OS, which exhibited superior discriminative power (AUCs were 0.811 and 0.795).

Conclusions: Our study established and validated a survival prognostic model system based on 4 unique immune related genes in ccRCC, which expands knowledge in tumor immune status and provide a potent prediction tool in future.

Keywords: Clear cell renal cell carcinoma (ccRCC); immunity; prognosis signature; tumor biomarkers; tumor microenvironment

Submitted Oct 18, 2020. Accepted for publication Feb 10, 2021.
doi: 10.21037/tau-20-1348
View this article at: http://dx.doi.org/10.21037/tau-20-1348

Introduction

Clear cell renal cell carcinoma (ccRCC) representing approximately 75% of RCC cases with more than 175000 deaths per year (1). Although surgical resection is effective for localized RCC, about one-third cases suffered recurrences and metastases with worse prognosis (2). Various molecular signatures of ccRCC implies that distinct survival advantages exist in the certain subtypes (3,4). Owing to heterogeneity, discovering reliable molecular biomarkers can help to improve prognostic determination and guide clinical decision. Actually, RCC is believed to be an immunogenic tumor for long time. Interleukin 2 (IL-2) and interferon alpha (IFN-a) were used for therapeutic regimens for advanced RCC in the 1990s to early 2000s, and the incidence of complete remission was about 3–5% (5,6). Recently, trail of KEYNOTE-426 and JAVELIN Renal 101 demonstrates using PD-1 immune checkpoint inhibitor-based combination regimens as the first line setting can significantly improve advanced RCC survival, which have been approved by FDA (7,8). Therefore, further exploration of immune related molecular network in RCC definitely helps to develop comprehensive understanding of immune evasion and provide insights into making therapeutic strategy. Immune molecular regulation is the key mechanism for host innate immunity and immune surveillance. It is necessary to explore clinical significance of immune-related biomarkers, especially immune-related genes (IRGs) which could predict prognosis of patients, and potentially portrait tumor microenvironment (TME) (9,10).

In this study, we identified 4 immune-related genes (*CRABP2*, *LTB4R*, *PTGER1* and *TEK*) through integrated analyses of mRNA expression data from TCGA database and independently assessed. Multivariate Cox proportional hazards models were constructed by 4 genes and validated the accuracy in an external ICGC dataset. Moreover, we investigated a high proportion of CD8 T cell, regulatory T cell and NK cell in the unfavorable-risk group. High levels of immune response suppressors (PD-1, CTLA4, TNFRSF9, TIGIT and LAG3) were observed in unfavorable-risk group and positively correlated with risk score. According to aforementioned data, a nomogram was well established for clinical use and also externally validated its superior power by ICGC data.

We present the following article in accordance with the TRIPOD reporting checklist (available at http://dx.doi.org/10.21037/tau-20-1348).

Methods

Study design and dataset information

The work flow of our study is shown in *Figure 1*. The expression profile and clinical data of 539 ccRCC patients in TCGA-KIRC dataset were downloaded from TCGA portal (online URL: https://cdn.amegroups.cn/static/public/tau-20-1348-1.pdf) and 91 RCC patients from ICGC database were downloaded from ICGC portal (online URL: https://dcc.icgc.org/). Immune-related genes list was downloaded from the ImmPort database (online URL: https://www.immport.org/home/). All data were preprocessed in R software (online URL: https://www.r-project.org/; version 3.6.0;). 518 patients in TCGA-KIRC cohort and 91 patients in ICGC cohort with clinical information (Table S1 and S2) were screened for subsequent analyses. All procedures performed in this study were in accordance with the Declaration of Helsinki (as revised in 2013).

Identification of IRDEGs in TCGA-KIRC dataset

Differential analysis was conducted in TCGA-KIRC dataset through limma package (11,12), with the following cut-off: adjusted P value <0.05 and absolute $\log_2$FC >1.5. The differentially expressed genes list and immune-related genes list from the ImmPort database were uploaded into the Venn diagram online software (online URL: http://bioinformatics.psb.ugent.be/webtools/Venn/) to obtain the IRDEGs. The heatmap of IRDEGs expression was performed by pheatmap package.

Construction and validation of the risk model

518 patients in TCGA-KIRC dataset were included as a training set while 91 patients in the ICGC database were assigned as a validation set. Univariate Cox proportional hazards regression analysis was applied to identify the significant prognostic factors associated with OS, and Lasso regression was used to exclude overfitting genes. The candidate genes were analyzed in a multivariate Cox proportional hazards regression analysis to estimate their relative contributions to survival prediction. Subsequently, a prognostic model was constructed: risk score = expression of $gene_1 \times \beta 1$ + expression of $gene_2 \times \beta 2$ +…… + expression of $gene_n \times \beta n$ (13,14). According to the median risk score, patients were divided into two groups (favorable-risk

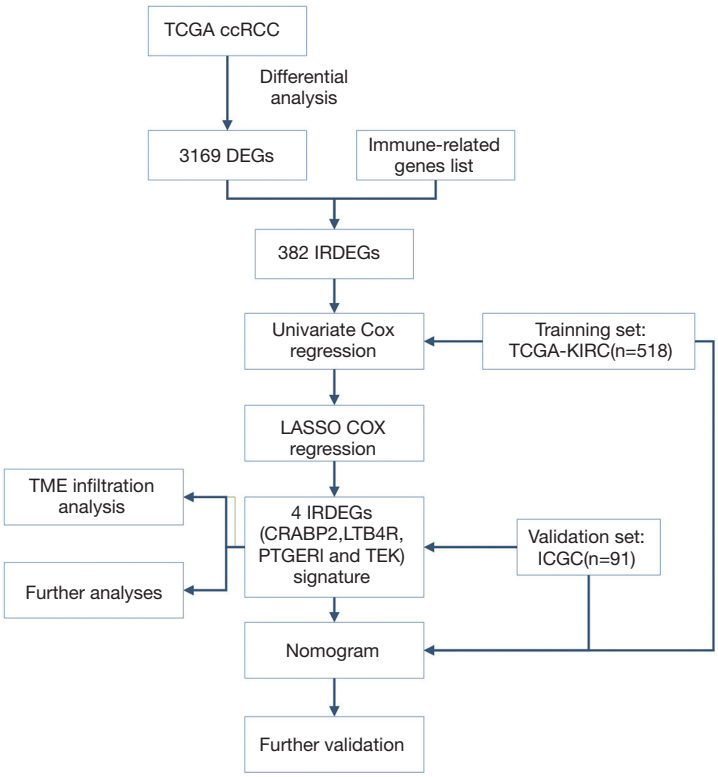

Figure 1 The workflow of our research project. Differential analysis was conducted in TCGA-KIRC dataset to obtain differentially expressed with the following cut-off: adjusted P value <0.05 and absolute log2FC >1.5; 382 immune-related genes were identified after taking intersection of the lists of DEGs and IRGs; 4 IRDEGs (*CRABP2*, *LTB4R*, *PTGER1* and *TEK*) were finally identified and used to constructed a prognostic model after univariate cox and LASSO cox analyses. Further analyses were conducted to validate the robustness of model and explored the potential mechanism.

group and unfavorable-risk group), and we applied the Kaplan-Meier and log-rank methods to test whether the survival distribution of different groups was equal. Receiver operating characteristic (ROC) curves were used to assess the predictive value of the risk model according to the areas under the respective ROC curves (AUCs). Time-dependent ROC curve analysis was conducted by using the survival ROC package (15).

RNA extraction and qRT-PCR analysis

Total RNA of 35 pairs of ccRCC and normal tissues RNA were extracted using a Trizol reagent, and 500 ng of RNA was used to synthesize cDNA, and qRT-PCR was performed on ABI system. The primer sequences are listed in Table S3.

Estimation of TME infiltration between groups

CIBERSORT, a deconvolution algorithm to characterize different cell compositions of the samples based on the immune gene signature sets, including 547 genes and 22 immune cell subtypes (16). We downloaded the result of 518 patients in TCGA cohort calculated by CIBERSORT algorithm from TIMER 2.0(Online URL: http://timer.cistrome.org/) (17) to estimate the infiltration of 22 different immune cell subtypes in the TME for further investigation of the composition and difference between favorable-risk and unfavorable-risk group. Each sample had been calculated a proportion in each cell subtype to estimate the relative abundance of TME immune infiltrating cells. Wilcox test was applied to compare the infiltration proportion of the 22 cell types between the unfavorable-risk group and the favorable-risk group.

Construction and validation of the clinical nomogram

We constructed a nomogram, which was widely used to predict the survival probability of patients in clinical (18), with the incorporation of age, gender, TNM stage, Fuhrman grade, necrosis and risk score through R rms package. We also used ROC curves to evaluate the predictive performance of nomogram at 1-, 3- and 5-year. In addition, calibration curves were used to evaluate the accuracy of the predicted survival time for 3- and 5-year OS, and decision curve analysis (DCA) was performed to evaluate the clinical application benefit between different variables.

Statistical analysis

All statistical analyses were performed by R software with the cut-off of P<0.05. Univariate and multivariate Cox proportional hazards regression analyses were used for identifying of prognosis-related IRDEGs and independent prognostic factors. Spearman correlation test was applied to analyze the correlation between the risk score and the expression of immune checkpoint genes. Survival data were calculated using the Kaplan-Meier method and the log-rank test. The relative expression level of four IRDEGs was analyzed by paired *t* test.

Results

Identification of IRDEGs in ccRCC

After differential analysis in TCGA-KIRC cohort, 3,169 DEGs were detected (adjusted P value <0.05 and absolute $\log_2$FC >1.5), among which 1,635 genes were upregulated, and 1534 genes were downregulated (*Figure 2A*). Taking the intersection of DEGs and the immune-related genes list, 382 IRDEGs were identified (*Figure 2B*), with 253 IRDEGs upregulated and 129 IRDEGs downregulated. The heatmap to visualize the expression of 382 IRDEGs in normal samples and tumor samples is shown in *Figure 2C*, and the result of differential analysis are shown in https://cdn.amegroups.cn/static/public/tau-20-1348-2.xlsx and Table S4.

Construction of prognostic model in TCGA cohort

175 IRDEGs was calculated to be significantly associated with OS after univariate Cox regression analysis (P<0.05) (Table S5). Lasso regression was used to filter genes to obtain 8 candidate genes (*Figure 2D,2E*), which were subsequently included in the multivariate Cox regression analysis. A prognostic gene signature consisting of 4 genes was ultimately constructed with the P value <0.05 in multivariate Cox regression analysis (*Table 1* and Table S6). Among these 4 genes, *TEK* was identified as a protective gene because of its hazard ratios (HR) value of <1, while *CRABP2*, *LTB4R* and *PTGER1* were considered to be predictive genes of poor prognosis. Based on the analysis result, we constructed a computational formula: risk score = (0.074× expression level of *CRABP2*) + (0.165× expression level of *LTB4R*) + (0.052× expression level of *PTGER1*) + (-0.203× expression level of *TEK*), and the expression level was obtained by the log2-transformed FPKM+1 of each gene. Subsequently, a total of 518 patients in TCGA cohort were divided into two groups (unfavorable-risk group and favorable-risk group) according to the median risk score. *Figure 3A* shows the distribution of risk scores, patient survival status and the four gene expression levels in the 518 patients, which were sorted by the risk score of the four-gene signature. As the risk score increasing, the expression of the 4 IRDEGs also changed accordingly, and the prognosis of patients also became worse. Besides, as *Figure 3B* and *3C* show, there were obvious differences in both OS and PFS between the two groups (P<0.0001). On the other hand, a time-dependent ROC was used to assess the prognostic value of the four-gene signature in the training set. The AUCs of the signature were respectively 0.744, 0.734, and 0.753 for the 1-, 3- and 5-year OS (*Figure 3D*) while for the 1-, 3- and 5-year PFS were 0.696, 0.711, and 0.734(*Figure 3E*), indicating our risk model had a good performance on predicting prognosis. Besides, further analysis showed risk score was an independent prognostic factor (HR: 3.137; 95% CI: 2.383-4.131; P<0.001) (*Table 1*).

External validation of prognostic model in ICGC cohort

We used the data from ICGC database as an external validation (*Figure 4*). The distribution of risk scores and survival status of patients, as well as the expression level of the 4 IRDEGs in ICGC cohort, were shown in *Figure 4A* and it was observed that the expression had an obvious difference between unfavorable-risk group and favorable-risk group. Besides, Kaplan-Meier analysis indicated that unfavorable-risk group was significantly associated with a poor prognosis (P<0.05), consistently with the above results (*Figure 4B*). And the AUCs of ROC analysis were respectively 0.635, 0.638 and 0.635 at 1-, 3- and 5-year OS value, indicating the stability of risk model in different cohorts (*Figure 4C*).

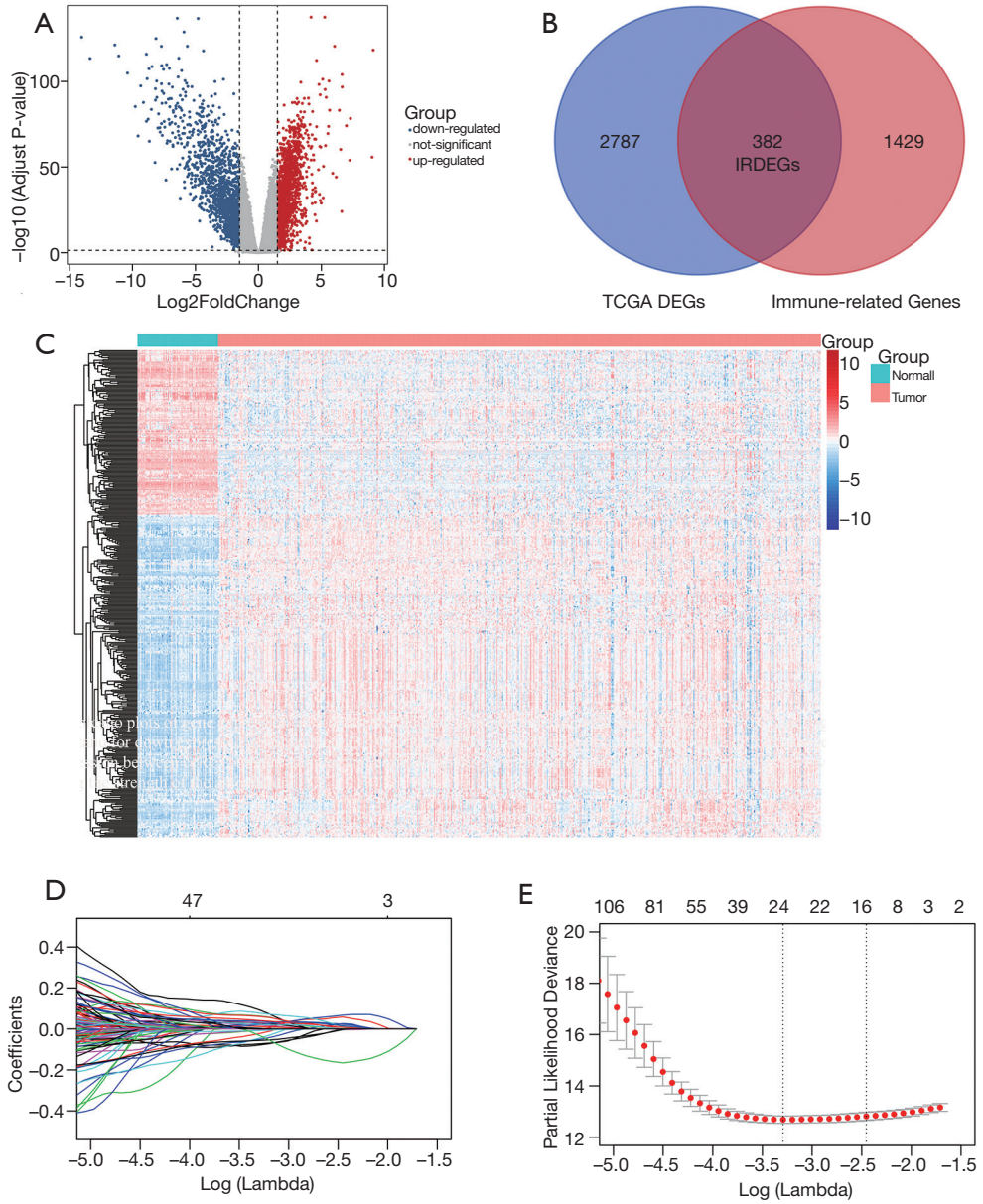

Figure 2 Differential analysis of TCGA-KIRC cohort and LASSO regression. (A) The volcano plot of TCGA-KIRC cohort. Red plots represent upregulated genes while blue plots represent downregulated genes both with adj.P <0.05. (B) Venn diagram of DEGs and IRGs. (C) The heatmap of 382 IRDEGs in ccRCC and normal samples. Each column represents one sample and each row represents one gene. The gradual color ranging from blue to red represents the changing process from down to up regulation. (D) Plot of LASSO coefficient profiles. (E) Plot of partial likelihood deviance for the 382 IRDEGs.

Table 1 Univariate analysis and Multivariate analysis of the 4 IRGs and signature

	Univariate analysis		Multivariate analysis		
	HR (95% CI)	P value	HR (95% CI)	P value	Coefficient
Gene symbol					
CRABP2	1.077 (1.001–1.158)	0.0508	0.672	0.0210	–0.3979
LTB4R	1.180 (1.001–1.390)	0.0029	1.217	0.0300	0.1961
PTGER1	1.054 (1.008–1.102)	P<0.001	1.199	0.0200	0.1816
TEK	0.639 (0.711–0.936)	P<0.001	0.754	0.0150	–0.2817
Factors					
Age	1.030 (1.016–1.043)	P<0.001	1.031(1.016–1.045)	P<0.001	
Stage		P<0.001			
I	Reference		Reference		
II	1.273 (0.683–2.371)		1.230 (0.657–2.304)	0.518	
III	2.656 (1.755–4.019		1.937 (1.272–2.952)	0.002	
IV	6.685 (4.537–9.851)		5.239 (3.524–7.787)	P<0.001	
Four-gene signature			3.137 (2.383–4.131)	P<0.001	

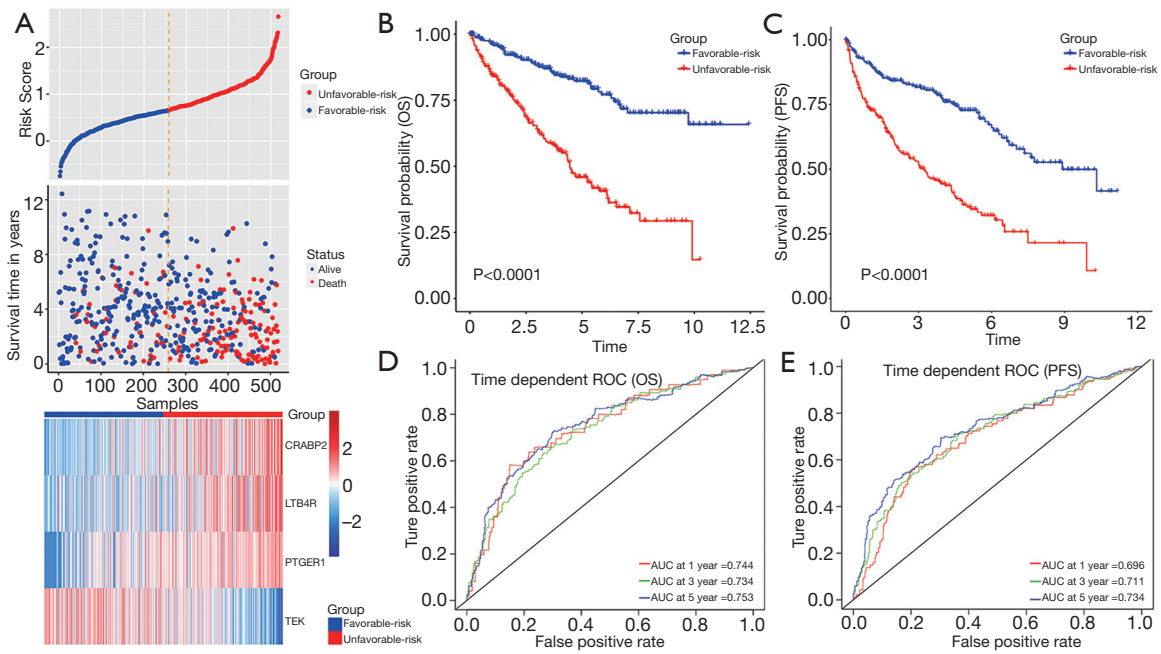

Figure 3 The 4-IRG prognostic signature in the ccRCC patients (TCGA cohort). (A) From top to bottom are the risk score distribution, the patients' survival status distribution, and the heatmap of the 4 genes for low and unfavorable-risk groups, in which each column represents one sample and each row represents one gene. (B, C) The Kaplan-Meier curves of OS and PFS for low and unfavorable-risk groups. (D, E) The ROC curves for predicting OS and PFS in training set by the risk score and the AUC of 1, 3, 5-year.

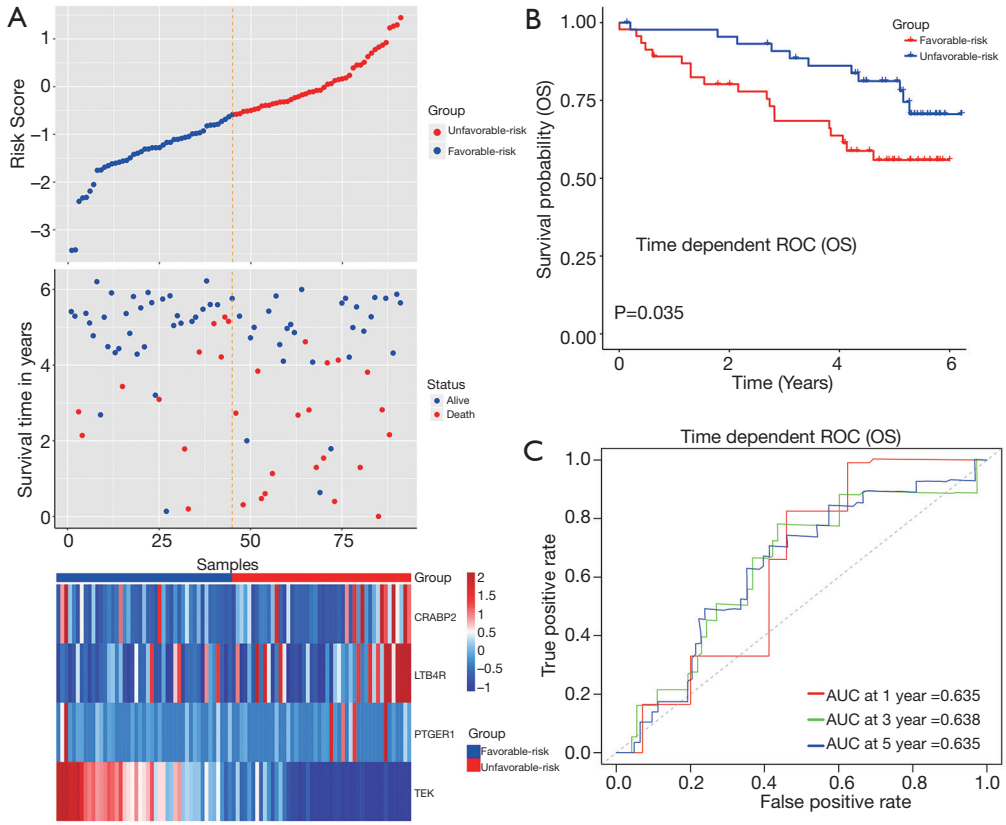

Figure 4 The 4-IRG prognostic signature in the ICGC cohort. (A) From top to bottom are the risk score distribution, the patients' survival status distribution, and the heatmap of the 4 genes for low and unfavorable-risk groups (B) The Kaplan-Meier curves for low and unfavorable-risk groups. (C) The ROC curves for predicting OS in validation set by the risk score and the AUC of 1, 3, 5-year.

Validation in clinical samples

We used 35 pairs of ccRCC (Table S7) and normal tissues to detect the expression of the four IRDEGs. The results showed LTB4R was high expressed in ccRCC compared with normal tissues, and CRABP2, PTGER1, TEK were low expressed, consistent with the expression data of TCGA database (*Figure 5*).

TME immune cell infiltration analysis and immune checkpoints analysis

We summarized the result of 518 ccRCC patients calculated by CIBERSORT algorithm (Figure S1) and compared all the immune cell subtypes in two groups (Table S8). Infiltration proportion of partial cell subtypes have an obvious difference between two groups, among which mainly CD8 T cell, follicular helper T cell, regulatory T cell, activated NK cell, M0 Macrophage have a higher infiltration proportion in the unfavorable-risk group, while M1 Macrophage, M2 Macrophage and other cell types have a lower proportion (*Figure 6A*). We further explored the expression of the T cell exhaustion-related markers and immunomodulators (PD-1, CTLA4, TNFRSF9, TIGIT, LAG3) in two groups and found all markers in the unfavorable-risk group were upregulated, indicating an immunosuppressive and exhausted phenotype in the unfavorable-risk group (*Figure 6B*). Subsequent correlation analysis also showed a positive correlation between risk score and the above markers (*Figure 6C*). Based on the above analyses, we found two groups had a significant distinct pattern of immune infiltration, which may lead to different survival benefits.

Construction and validation of the nomogram

We constructed a nomogram containing age, gender, TNM stage, Fuhrman grade, necrosis and risk score to

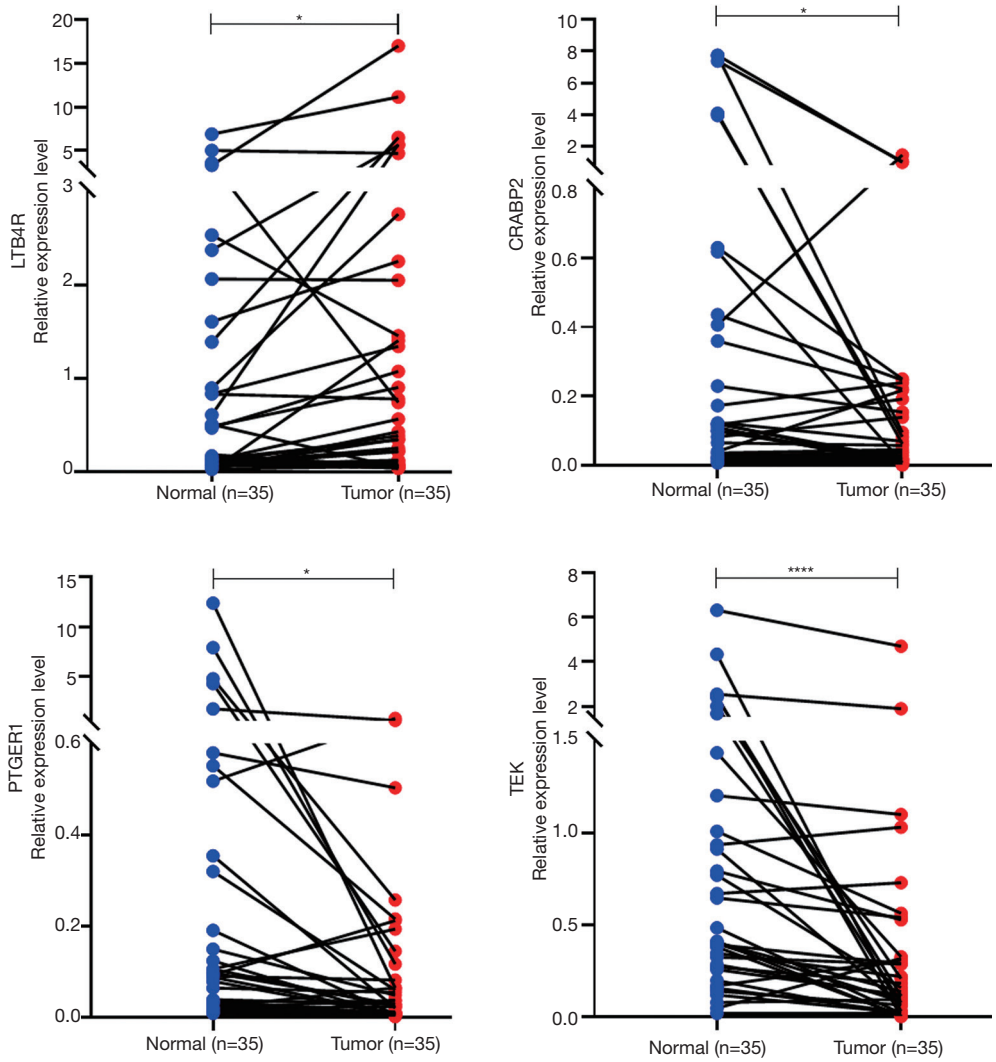

Figure 5 Relative expression level of the 4 IRGs in paired ccRCC and normal tissues.

predict 3- and 5-year survival probability. Each variable had a corresponding score (Table S9), and an overall score could be finally calculated to predict the survival probability at the corresponding time (*Figure 7A*). To validate the performance of nomogram, we conducted the ROC analysis, and the result showed respective AUCs were 0.811 and 0.795 in the TCGA cohort (*Figure 7B*). The calibration curves showed good consistency between the actual and predicted outcomes of 3- and 5-year OS (*Figure 7C*). Decision curve analysis (DCA) was also conducted, and all variable curves were above the two solid curves. The curve of the nomogram was above the curve of risk score at 3- and 5-year (*Figure 7D*), indicating nomogram had a better clinical net benefit. We also constructed another nomogram containing age, gender, TNM stage, and risk score. And the AUCs were 0.811, 0.786 while in the validation set were 0.728, 0.713 at 3-, 5-year, suggesting its stability and effectiveness (Figures S2, S3). Calibration curves and DCA also showed the robustness of our nomogram.

Discussion

Immune related genes (IRGs) play an important role in tumor immune infiltration as well as tumor progression in ccRCC (19,20) and strongly influence complicate soluble factors secretion, which correlate with therapeutic response and clinical outcome (21). IRGs based prognostic model have been successfully developed for hepatocellular,

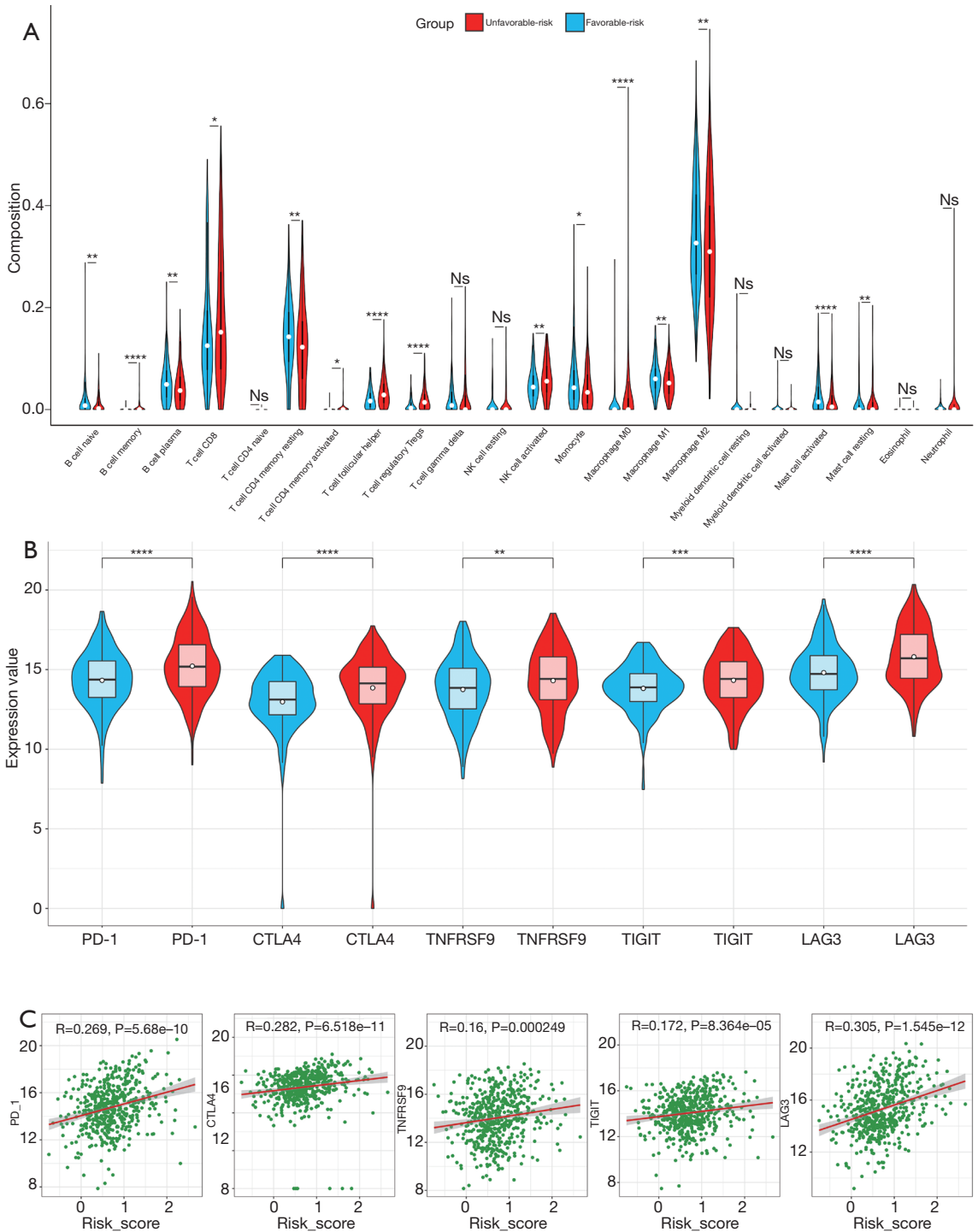

Figure 6 TME immune cell infiltration characteristics of 22 immune cell subtypes in unfavorable-risk and favorable-risk groups. (A) The violin plot of the abundance of immune cell subtypes in two groups. The asterisks on the top represented the P value of Wilcoxon test (ns P>0.05; *P<0.05; **P<0.01; ***P<0.001; ****P<0.0001). (B) The violin plot of the expression of T cell exhaustion-related markers and common immune checkpoint in two groups. (C) Spearman correlation analysis of risk score and above markers.

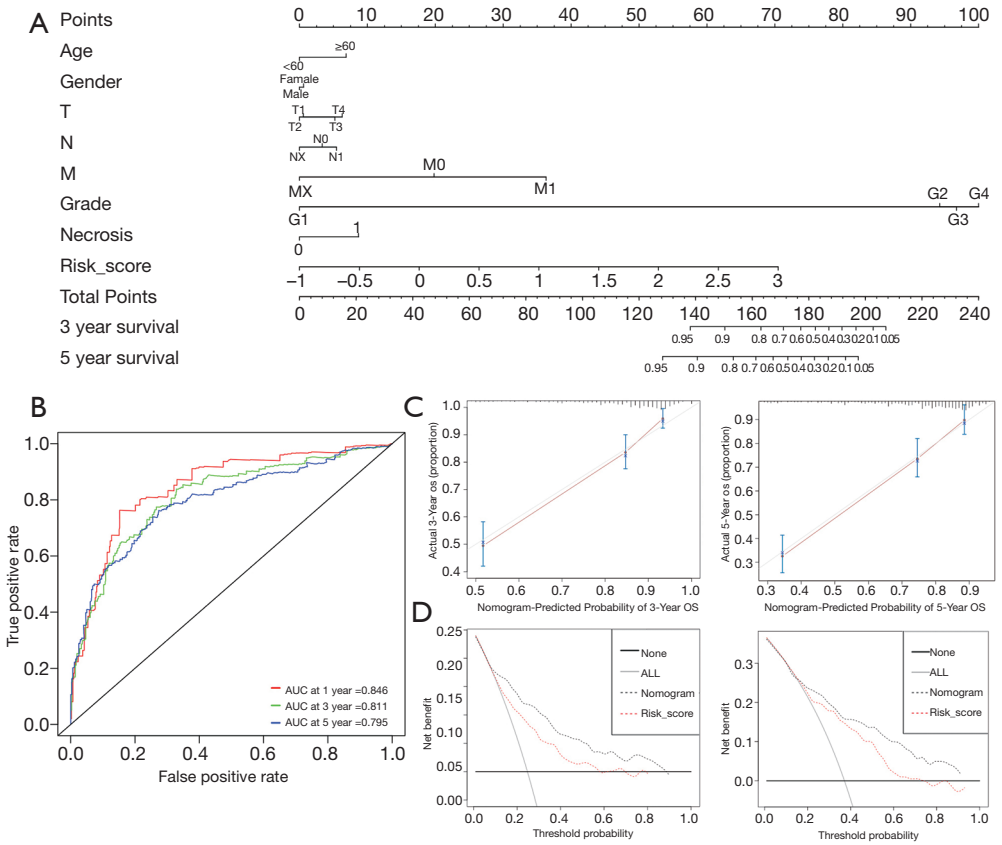

Figure 7 Construction and validation of the nomogram in TCGA-KIRC cohort. (A) The clinical nomogram of the ccRCC patients (TCGA cohort). (B) The ROC curves of nomogram for predicting OS in training set and the AUC of 1, 3, 5-year. (C) The 3-year and 5-year calibration curves of the nomogram in training set. (D) The 3-year and 5-year DCA plots of the nomogram. The grey, red dotted lines respectively represent net benefits of nomogram and risk score at different threshold probabilities.

colorectal, lung and bladder cancers (22-25). In this study, we screened and validated *CRABP2*, *LTB4R*, *PTGER1* and *TEK* from TCGA database as potent IRGs to predict the survival risk in ccRCC patients. Multivariate Cox proportional hazards models were constructed to stratify patients based on the 4 genes signature. Laboratory q-PCR confirmed LTB4R upregulated and CRABP2, PTGER1, TEK downregulated in 35 pairs of ccRCC and normal tissues.

LTB4R is a receptor of Leukotriene B4 and is expressed mainly in leukocytes like granulocytes, macrophages and eosinophils (26). Several studies implied it was involved in CD8 T cells recruiting (27,28). The neutrophilic influx induced by LTB4 increases the pro-tumorigenic activity of tumor-associated neutrophils through releasing reactive oxygen species, inflammatory cytokines and injuring innate immune response (29,30). CRABP2 was responding in retinoic acid (RA) transduction as a tumor suppressive pathway (31). However, artificially overexpressing CRABP2 in Caki-2 cells did not exhibit a significant change in RA sensitivity. Our data indicated CRABP2 was lowly expressed in ccRCC samples, which was consistent with previous study (32). Although the exactly role of CRABP2 in RCC is not clear yet, our data showed high CARBP2 expression was an independent predictor factor for worse prognosis. Further investigations are necessary to define other molecules involved in CARBP2 mediated RA signaling and metabolism in RCC. PTGER1 is one of the receptors of prostaglandin and it couples with G-proteins to activate protein kinase C (33). Previous study implied blocking PTGER1 could suppress immunosuppressive function of Treg and subsequently inhibit tumor growth in colon cancer (34). In ccRCC, our result also exhibited high PTGER1 expression was correlated with worse prognosis.

TEK encodes Tie2, which cooperate with VEGFs as critical regulators of vascular development (35). Actually, mechanisms of angiogenesis are extremely complex depending on different tumor stage and content, therefore, the prediction role of Tie2 is inconsistent among different tumor types (36). Increasing Tie2 expression correlated with high metastasis risk and poor survival among breast cancer and glioblastoma patients (37,38). However, in ccRCC, our data implied downregulation of TEK associated with a poor prognosis which was also demonstrated in previous studies (39,40). Low expression of TEK has been noted in aggressive ccRCC for years (41). Recently, when compared gene prevalence between nonmetastatic and metastatic ccRCC by target next generation sequencing from 106 sporadic cases, higher frequencies of *TEK* mutations involved in metastatic cohort (42). Since Tie2 signaling influences vascular permeability, low expression of Tie2 may potentiate inflammatory cells migration into tumor microenvironment (43). Inflammatory cytokines such as TNF-α, IL-6, CXCL8 induces a more aggressive tumor phenotype via immune surveillance and form premetastatic niche. Overall, we assume TEK is a tumor suppressor in ccRCC, further studies are needed in future.

Solid tumors usually disrupt tumor target immune response by subvert immune surveillance. Tumor immune signature is highly correlated with tumor prognosis and response to immunotherapy. When using a 34-gene expression signature, ccRCC can be characterized into high angiogenesis tumor with improved prognosis or high immunocytes tumor with worse survival (44). Tumor infiltrating lymphocytes in ccRCC were analyzed by gene expression and cytometry phenotyping, the result implied more poorly cytotoxic CD8 T cell, Treg infiltrate in unfavorable risk group (45). In this current study, we also investigated high proportion of CD8 T cell, Treg, NK cell in unfavorable risk group through CIBERSORT algorithm, which indicated that our novel prediction model could properly distinct patient into different immunological features. Besides, a group of immunomodulators (PD-1, CTLA4, TNFRSF9, TIGIT and LAG3) was significantly correlated with our risk score, and confirmed our risk model stably stratified patients from immune evasion perspective.

In order to increase prediction accuracy, we developed a clinical nomogram with age, gender, TNM stage, Fuhrman grade, necrosis and risk score. This nomogram obtained an AUC of 0.846, 0.811 and 0.795 in predicting the possibility of survival at 1-, 3- and 5-year respectively. As there is lack of Fuhrman grade, necrosis information in ICGC database, we removed these two factors from original nomogram for validation. The modified nomogram consistently obtained a relatively high AUC of 0.755, 0.728 and 0.713 in survival prediction at 1-, 3- and 5-year separately in ICGC data. Hence, based on the 4 immune related genes *CRABP2*, *LTB4R*, *PTGER1 and TEK*, we successfully constructed a prognostic risk model for ccRCC and externally validated its accuracy. Defective T-cells and aberrant expression suppressive immunomodulators lead tumor be more aggressive. Owing to data we obtained from public database, further independent validation in prospective studies is needed.

Acknowledgments

English Language Editor: Dr. M. Mumin.
Funding: Our work was supported by National Natural Science Foundation of China (No. 81202011, 81572522); Science and Technology Planning Project of Guangdong Province, China (No. 2016A020215235); Pearl River Nova Program of Guangzhou, China (No. 201710010057).

Footnote

Reporting Checklist: The authors have completed the TRIPOD reporting checklist. Available at http://dx.doi.org/10.21037/tau-20-1348

Data Sharing Statement: Available at http://dx.doi.org/10.21037/tau-20-1348

Peer Review File: Available at http://dx.doi.org/10.21037/tau-20-1348

Conflicts of Interest: All authors have completed the ICMJE uniform disclosure form (available at http://dx.doi.org/10.21037/tau-20-1348). The authors have no conflicts of interest to declare.

Ethical Statement: The authors are accountable for all aspects of the work in ensuring that questions related to the accuracy or integrity of any part of the work are appropriately investigated and resolved. All procedures performed in this study were in accordance with the Declaration of Helsinki (as revised in 2013).

References

1. Bray F, Ferlay J, Soerjomataram I, et al. Global cancer statistics 2018: GLOBOCAN estimates of incidence and mortality worldwide for 36 cancers in 185 countries. CA Cancer J Clin 2018;68:394-424.
2. Gupta K, Miller JD, Li JZ, et al. Epidemiologic and socioeconomic burden of metastatic renal cell carcinoma (mRCC): a literature review. Cancer Treat Rev 2008;34:193-205.
3. Rini B, Goddard A, Knezevic D, et al. A 16-gene assay to predict recurrence after surgery in localised renal cell carcinoma: development and validation studies. Lancet Oncol 2015;16:676-85.
4. Brooks SA, Brannon AR, Parker JS, et al. ClearCode34: A prognostic risk predictor for localized clear cell renal cell carcinoma. Eur Urol 2014;66:77-84.
5. Bukowski RM. Natural history and therapy of metastatic renal cell carcinoma: the role of interleukin-2. Cancer 1997;80:1198-220.
6. Motzer RJ, Bacik J, Murphy BA, et al. Interferon-alfa as a comparative treatment for clinical trials of new therapies against advanced renal cell carcinoma. J Clin Oncol 2002;20:289-96.
7. Rini BI, Plimack ER, Stus V, et al. Pembrolizumab plus Axitinib versus Sunitinib for Advanced Renal-Cell Carcinoma. N Engl J Med 2019;380:1116-27.
8. Motzer RJ, Penkov K, Haanen J, et al. Avelumab plus Axitinib versus Sunitinib for Advanced Renal-Cell Carcinoma. N Engl J Med 2019;380:1103-15.
9. Chen YP, Wang YQ, Lv JW, et al. Identification and validation of novel microenvironment-based immune molecular subgroups of head and neck squamous cell carcinoma: implications for immunotherapy. Ann Oncol 2019;30:68-75.
10. Ji RR, Chasalow SD, Wang L, et al. An immune-active tumor microenvironment favors clinical response to ipilimumab. Cancer Immunol Immunother 2012;61:1019-31.
11. Phipson B, Lee S, Majewski IJ, et al. Robust Hyperparameter Estimation Protects against Hypervariable Genes and Improves Power to Detect Differential Expression. Ann Appl Stat 2016;10:946-63.
12. Ritchie ME, Phipson B, Wu D, et al. limma powers differential expression analyses for RNA-sequencing and microarray studies. Nucleic Acids Res 2015;43:e47.
13. Huang R, Liao X, Li Q. Identification and validation of potential prognostic gene biomarkers for predicting survival in patients with acute myeloid leukemia. Onco Targets Ther 2017;10:5243-54.
14. Zhou M, Zhao H, Wang Z, et al. Identification and validation of potential prognostic lncRNA biomarkers for predicting survival in patients with multiple myeloma. J Exp Clin Cancer Res 2015;34:102.
15. Heagerty PJ, Zheng Y. Survival model predictive accuracy and ROC curves. Biometrics 2005;61:92-105.
16. Newman AM, Liu CL, Green MR, et al. Robust enumeration of cell subsets from tissue expression profiles. Nat Methods 2015;12:453-7.
17. Li T, Fan J, Wang B, et al. TIMER: A Web Server for Comprehensive Analysis of Tumor-Infiltrating Immune Cells. Cancer Res 2017;77:e108-10.
18. Balachandran VP, Gonen M, Smith JJ, et al. Nomograms in oncology: more than meets the eye. Lancet Oncol 2015;16:e173-80.
19. Xu WH, Shi SN, Xu Y, et al. Prognostic implications of Aquaporin 9 expression in clear cell renal cell carcinoma. J Transl Med 2019;17:363.
20. Du GW, Yan X, Chen Z, et al. Identification of transforming growth factor beta induced (TGFBI) as an immune-related prognostic factor in clear cell renal cell carcinoma (ccRCC). Aging (Albany NY) 2020;12:8484-505.
21. Wu T, Dai Y. Tumor microenvironment and therapeutic response. Cancer Lett 2017;387:61-8.
22. Luo C, Lei M, Zhang Y, et al. Systematic construction and validation of an immune prognostic model for lung adenocarcinoma. J Cell Mol Med 2020;24:1233-44.
23. Qiu H, Hu X, He C, et al. Identification and Validation of an Individualized Prognostic Signature of Bladder Cancer Based on Seven Immune Related Genes. Front Genet 2020;11:12.
24. Wang Z, Zhu J, Liu Y, et al. Development and validation of a novel immune-related prognostic model in hepatocellular carcinoma. J Transl Med 2020;18:67.
25. Zhao X, Liu J, Liu S, et al. Construction and Validation of an Immune-Related Prognostic Model Based on TP53 Status in Colorectal Cancer. Cancers (Basel) 2019;11:1722.
26. Tager AM, Luster AD. BLT1 and BLT2: the leukotriene

B(4) receptors. Prostaglandins Leukot Essent Fatty Acids 2003;69:123-34.
27. Chheda ZS, Sharma RK, Jala VR, et al. Chemoattractant Receptors BLT1 and CXCR3 Regulate Antitumor Immunity by Facilitating CD8+ T Cell Migration into Tumors. J Immunol 2016;197:2016-26.
28. Sharma RK, Chheda Z, Jala VR, et al. Expression of leukotriene B(4) receptor-1 on CD8(+) T cells is required for their migration into tumors to elicit effective antitumor immunity. J Immunol 2013;191:3462-70.
29. Galdiero MR, Garlanda C, Jaillon S, et al. Tumor associated macrophages and neutrophils in tumor progression. J Cell Physiol 2013;228:1404-12.
30. Fridlender ZG, Sun J, Kim S, et al. Polarization of tumor-associated neutrophil phenotype by TGF-beta: "N1" versus "N2" TAN. Cancer Cell 2009;16:183-94.
31. Fu YS, Wang Q, Ma JX, et al. CRABP-II methylation: a critical determinant of retinoic acid resistance of medulloblastoma cells. Mol Oncol 2012;6:48-61.
32. Goelden U, Pfoertner S, Hansen W, et al. Expression and functional influence of cellular retinoic acid-binding protein II in renal cell carcinoma. Urol Int 2005;75:269-76.
33. Sugimoto Y, Narumiya S. Prostaglandin E receptors. J Biol Chem 2007;282:11613-7.
34. O'Callaghan G, Ryan A, Neary P, et al. Targeting the EP1 receptor reduces Fas ligand expression and increases the antitumor immune response in an in vivo model of colon cancer. Int J Cancer 2013;133:825-34.
35. Ramsauer M, D'Amore PA. Getting Tie(2)d up in angiogenesis. J Clin Invest 2002;110:1615-7.
36. Sharma S, Sharma MC, Sarkar C. Morphology of angiogenesis in human cancer: a conceptual overview, histoprognostic perspective and significance of neoangiogenesis. Histopathology 2005;46:481-9.
37. Dales JP, Garcia S, Bonnier P, et al. Tie2/Tek expression in breast carcinoma: correlations of immunohistochemical assays and long-term follow-up in a series of 909 patients. Int J Oncol 2003;22:391-7.
38. Zheng S, Tao W. Identification of Novel Transcriptome Signature as a Potential Prognostic Biomarker for Anti-Angiogenic Therapy in Glioblastoma Multiforme. Cancers (Basel) 2020;12:2368.
39. Shen C, Liu J, Wang J, et al. Development and validation of a prognostic immune-associated gene signature in clear cell renal cell carcinoma. Int Immunopharmacol 2020;81:106274.
40. Ha M, Son YR, Kim J, et al. TEK is a novel prognostic marker for clear cell renal cell carcinoma. Eur Rev Med Pharmacol Sci 2019;23:1451-8.
41. Kosari F, Parker AS, Kube DM, et al. Clear cell renal cell carcinoma: gene expression analyses identify a potential signature for tumor aggressiveness. Clin Cancer Res 2005;11:5128-39.
42. Meng H, Jiang X, Cui J, et al. Genomic Analysis Reveals Novel Specific Metastatic Mutations in Chinese Clear Cell Renal Cell Carcinoma. Biomed Res Int 2020;2020:2495157.
43. Parikh SM. Angiopoietins and Tie2 in vascular inflammation. Curr Opin Hematol 2017;24:432-8.
44. Iglesia MD, Parker JS, Hoadley KA, et al. Genomic Analysis of Immune Cell Infiltrates Across 11 Tumor Types. J Natl Cancer Inst 2016;108:djw144.
45. Giraldo NA, Becht E, Vano Y, et al. Tumor-Infiltrating and Peripheral Blood T-cell Immunophenotypes Predict Early Relapse in Localized Clear Cell Renal Cell Carcinoma. Clin Cancer Res 2017;23:4416-28.

Cite this article as: Liao Z, Yao H, Wei J, Feng Z, Chen W, Luo J, Chen X. Development and validation of the prognostic value of the immune-related genes in clear cell renal cell carcinoma. Transl Androl Urol 2021;10(4):1607-1619. doi: 10.21037/tau-20-1348

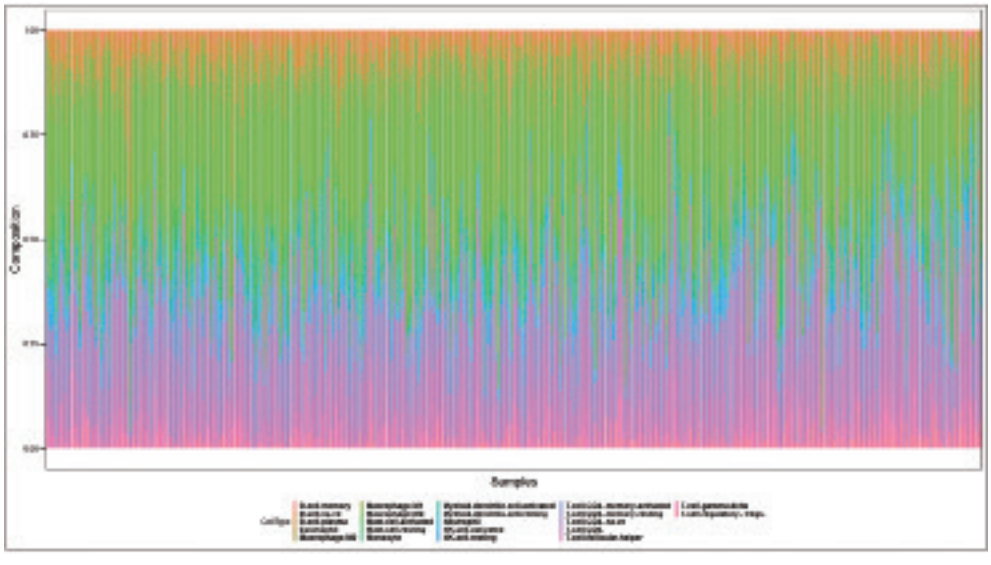

Figure S1 The summary of immune infiltration in 518 patients.

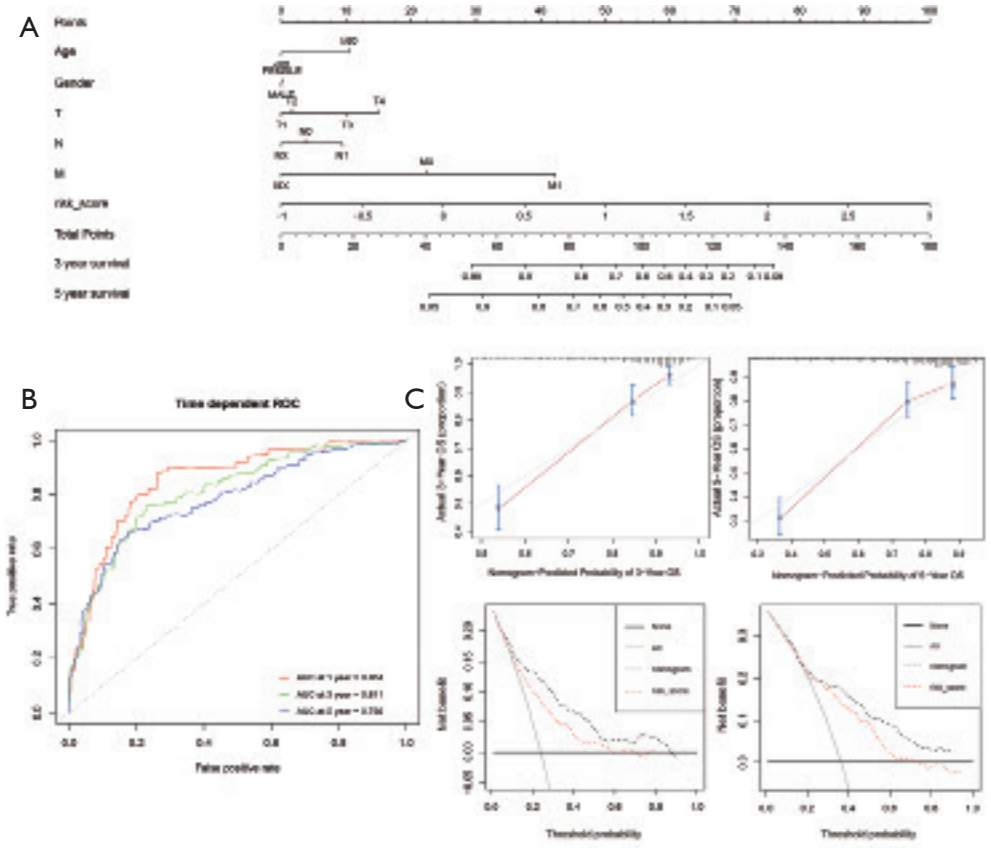

Figure S2 Construction and validation of the nomogram. (A) The clinical nomogram of the ccRCC patients (TCGA cohort). (B) The ROC curves of nomogram for predicting OS in training set and the AUC of 1, 3, 5-year. (C) The top line are the 3-year and 5-year calibration curves of the nomogram in training set; The bottom line are the 3-year and 5-year DCA plots of the nomogram.

http://dx.doi.org/10.21037/tau-20-1348

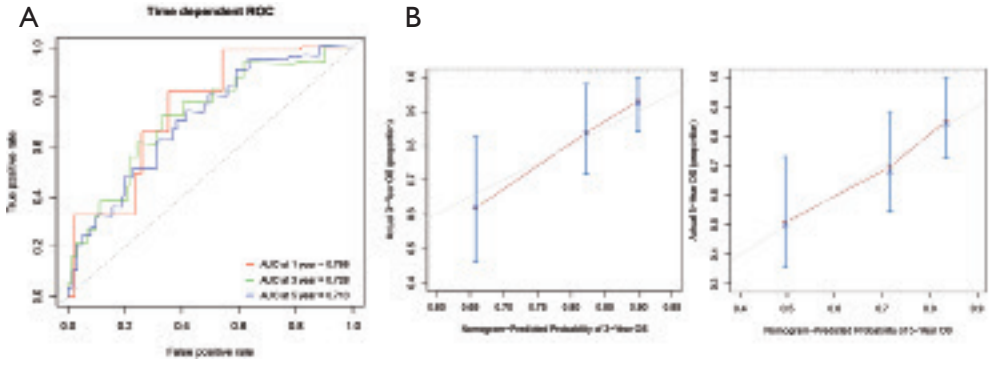

Figure S3 ROC curves for the nomogram in validation set (A) The ROC curves of nomogram for predicting OS in validation set and the AUC of 1, 3, 5-year. (B) 3-year and 5-year calibration curves of the nomogram in validation set.

Table S1 Clinical information for TCGA-KIRC dataset

Variable	No. of patients
Gender	
Male	335
Female	183
Age	
≥60	278
<60	240
Histological grade	
G1	13
G2	220
G3	204
G4	73
Gx	5
Not available	3
Stage	
I	257
II	56
III	123
IV	82
T stage	
I	263
II	68
III	176
IV	11
N stage	
N0	237
N1	15
Nx	266
M stage	
M0	430
M1	79
Mx	9

Table S2 Clinical information for ICGC dataset

Variable	No. of patients
Gender	
Male	52
Female	39
Age	
≥60	52
<60	39
Histological grade	
G1	13
G2	48
G3	15
G4	14
Not available	1
Stage	
I	53
II	13
III	16
IV	9
T stage	
I	54
II	13
III	22
IV	2
N stage	
N0	79
N1	2
Nx	10
M stage	
M0	81
M1	9
Mx	1

http://dx.doi.org/10.21037/tau-20-1348

Table S3 Primer sequences for qRT-PCR

CRABP2-F	ATCGGAAAACTTCGAGGAATTGC
CRABP2-R	AGGCTCTTACAGGGCCTCC
LTB4R-F	AGCTTTGTGGTGTGGAGTATCC
LTB4R-R	GCAACCAGCCAGTCCAAAAC
PTGER1-F	CACCTTCTTTGGCGGCTCTC
PTGER1-R	GATGCACGACACCACCATG
TEK-F	TCCGCTGGAAGTTACTCAAGA
TEK-R	GAACTCGCCCTTCACAGAAATAA

Table S4 Information for the 382 IRDEGs

Gene	Group
CD1D	Up-regulated gene
CD4	Up-regulated gene
CD8A	Up-regulated gene
CD8B	Up-regulated gene
CD74	Up-regulated gene
CTSE	Up-regulated gene
CTSS	Up-regulated gene
FCER1G	Up-regulated gene
HLA-A	Up-regulated gene
HLA-B	Up-regulated gene
HLA-DOB	Up-regulated gene
HLA-DPA1	Up-regulated gene
HLA-DPB1	Up-regulated gene
HLA-DQA1	Up-regulated gene
HLA-DQA2	Up-regulated gene
HLA-DQB1	Up-regulated gene
HLA-DRA	Up-regulated gene
HLA-DRB1	Up-regulated gene
HLA-F	Up-regulated gene
HLA-G	Up-regulated gene
HSPA2	Down-regulated gene
HSPA6	Up-regulated gene
IFNA14	Down-regulated gene
IFNG	Up-regulated gene
KIR2DL1	Up-regulated gene
KIR2DL3	Up-regulated gene
KIR2DL4	Up-regulated gene
KIR3DL1	Up-regulated gene
KIR3DL2	Up-regulated gene
KLRC1	Up-regulated gene
KLRC2	Up-regulated gene
KLRD1	Up-regulated gene
LTA	Up-regulated gene
PSMB8	Up-regulated gene
TAP1	Up-regulated gene
TAPBP	Up-regulated gene
KLRC4	Up-regulated gene
IFI30	Up-regulated gene
PROCR	Up-regulated gene
RAET1E	Down-regulated gene
RAET1L	Down-regulated gene
HAMP	Up-regulated gene
SLPI	Down-regulated gene
CXCL10	Up-regulated gene
CXCL9	Up-regulated gene
CXCL5	Up-regulated gene
CXCL11	Up-regulated gene
CXCL13	Up-regulated gene
XCL1	Up-regulated gene
DEFB1	Down-regulated gene
TMSB10	Up-regulated gene
LCN2	Down-regulated gene
BPI	Down-regulated gene
S100A8	Up-regulated gene
PTGDS	Down-regulated gene
PGLYRP2	Up-regulated gene
S100A2	Down-regulated gene
DEFB125	Down-regulated gene
DEFB132	Down-regulated gene
S100A5	Down-regulated gene
TMSB4Y	Down-regulated gene
TMSB15B	Up-regulated gene
S100Z	Up-regulated gene
S100A14	Down-regulated gene
AZU1	Up-regulated gene
WFDC2	Down-regulated gene
UMODL1	Down-regulated gene
TGFB1	Up-regulated gene
MMP9	Up-regulated gene
APOBEC3G	Up-regulated gene
FABP6	Up-regulated gene
NOD2	Up-regulated gene
MBL2	Up-regulated gene
TLR2	Up-regulated gene
PLAU	Down-regulated gene
PAEP	Up-regulated gene
LPA	Down-regulated gene
RBP4	Down-regulated gene
LTF	Down-regulated gene
FABP7	Up-regulated gene
FABP5	Up-regulated gene
OASL	Up-regulated gene
CRABP2	Down-regulated gene
CRABP1	Down-regulated gene
RBP2	Down-regulated gene
PMP2	Down-regulated gene
APOD	Down-regulated gene
PRTN3	Up-regulated gene
CYBB	Up-regulated gene
ISG20	Up-regulated gene
DUOX2	Down-regulated gene
IDO1	Up-regulated gene
SEMG1	Down-regulated gene
CCL20	Up-regulated gene
CHIT1	Up-regulated gene
CD40	Up-regulated gene
TLR7	Up-regulated gene
VEGFA	Up-regulated gene
ISG15	Up-regulated gene
TFR2	Up-regulated gene
IL27	Up-regulated gene
LYZ	Up-regulated gene
CCL5	Up-regulated gene
CCR6	Up-regulated gene
TLR8	Up-regulated gene
GNLY	Up-regulated gene
PDGFRA	Down-regulated gene
MSR1	Up-regulated gene
DLL4	Up-regulated gene
SLC11A1	Up-regulated gene
SEMG2	Down-regulated gene
DES	Down-regulated gene
TNFRSF10B	Up-regulated gene
CCL4	Up-regulated gene
APOBEC3H	Up-regulated gene
TMPRSS6	Up-regulated gene

Table S4 (*continued*)

Table S4 (*continued*)

http://dx.doi.org/10.21037/tau-20-1348

Table S4 (*continued*)

Gene	Group
MARCO	Up-regulated gene
KNG1	Down-regulated gene
KLRK1	Up-regulated gene
RNASE3	Up-regulated gene
IRF7	Up-regulated gene
LTB4R	Up-regulated gene
IL7R	Up-regulated gene
APOBEC3C	Up-regulated gene
PTGS2	Down-regulated gene
CD40LG	Up-regulated gene
CD14	Up-regulated gene
MASP1	Up-regulated gene
PROC	Down-regulated gene
HRG	Down-regulated gene
HMOX1	Up-regulated gene
STAB2	Up-regulated gene
PDCD1	Up-regulated gene
PCSK2	Down-regulated gene
ARG2	Down-regulated gene
AQP9	Up-regulated gene
FASLG	Up-regulated gene
APOH	Down-regulated gene
BIRC5	Up-regulated gene
VIM	Up-regulated gene
VCAM1	Up-regulated gene
GBP2	Up-regulated gene
ALB	Down-regulated gene
OAS1	Up-regulated gene
AGER	Up-regulated gene
NOS1	Down-regulated gene
CCL18	Up-regulated gene
CCL22	Up-regulated gene
CCR7	Up-regulated gene
CCR8	Up-regulated gene
CCL21	Down-regulated gene
CCL3	Up-regulated gene
CCL11	Down-regulated gene
CCR5	Up-regulated gene
CCL3L3	Up-regulated gene
CCL4L1	Up-regulated gene
XCL2	Up-regulated gene
CXCR4	Up-regulated gene
CXCR6	Up-regulated gene
FAM19A4	Down-regulated gene
FAM19A1	Down-regulated gene
CDH1	Down-regulated gene
IL10	Up-regulated gene
CRP	Up-regulated gene
PTGDR	Up-regulated gene
CD86	Up-regulated gene
HCK	Up-regulated gene
VDR	Down-regulated gene
OLR1	Up-regulated gene
RNASE2	Up-regulated gene
CD79A	Up-regulated gene
BTK	Up-regulated gene
VAV1	Up-regulated gene
RAC2	Up-regulated gene
CHP2	Down-regulated gene
CARD11	Up-regulated gene
CR2	Down-regulated gene
PIK3R5	Up-regulated gene
INPP5D	Up-regulated gene

Table S4 (*continued*)

Table S4 (*continued*)

Gene	Group
CD72	Up-regulated gene
LILRB3	Up-regulated gene
FCGR2B	Up-regulated gene
C3	Up-regulated gene
EDN1	Up-regulated gene
EDN3	Down-regulated gene
FGF10	Down-regulated gene
SEMA3B	Down-regulated gene
SEMA3D	Down-regulated gene
SEMA3E	Down-regulated gene
SEMA3G	Down-regulated gene
SEMA5B	Up-regulated gene
SEMA6A	Up-regulated gene
SEMA6B	Up-regulated gene
SEMA6D	Down-regulated gene
SLIT2	Down-regulated gene
TYMP	Up-regulated gene
CCR9	Down-regulated gene
CX3CR1	Up-regulated gene
CXCR3	Up-regulated gene
FPR1	Up-regulated gene
LTB4R2	Up-regulated gene
PLAUR	Up-regulated gene
PLXNA4	Down-regulated gene
PLXNB3	Up-regulated gene
PLXNC1	Up-regulated gene
PLXND1	Up-regulated gene
XCR1	Up-regulated gene
ADM	Up-regulated gene
ADM2	Up-regulated gene
AGRP	Down-regulated gene
AMH	Up-regulated gene
ANGPTL7	Down-regulated gene
APLN	Up-regulated gene
BDNF	Up-regulated gene
BMP1	Up-regulated gene
BMP3	Down-regulated gene
BMP5	Down-regulated gene
BMP6	Down-regulated gene
BMP7	Down-regulated gene
BTC	Down-regulated gene
CALCA	Down-regulated gene
CD70	Up-regulated gene
CGA	Down-regulated gene
CGB7	Up-regulated gene
CHGA	Down-regulated gene
CHGB	Down-regulated gene
CMTM3	Up-regulated gene
CMTM4	Down-regulated gene
EBI3	Up-regulated gene
EGF	Down-regulated gene
EPGN	Down-regulated gene
EPO	Up-regulated gene
ESM1	Up-regulated gene
FAM3B	Down-regulated gene
FGF1	Down-regulated gene
FGF20	Up-regulated gene
FGF7	Down-regulated gene
FGF9	Down-regulated gene
GDF6	Up-regulated gene
GDF7	Down-regulated gene
GDNF	Down-regulated gene
GMFG	Up-regulated gene

Table S4 (*continued*)

http://dx.doi.org/10.21037/tau-20-1348

Table S4 (*continued*)

Gene	Group
GNRH1	Up-regulated gene
GREM1	Down-regulated gene
GREM2	Down-regulated gene
IGF2	Down-regulated gene
IL11	Down-regulated gene
IL16	Up-regulated gene
IL19	Down-regulated gene
IL24	Up-regulated gene
IL32	Up-regulated gene
INHBB	Up-regulated gene
INHBE	Up-regulated gene
JAG2	Up-regulated gene
KITLG	Down-regulated gene
KL	Down-regulated gene
LEFTY2	Down-regulated gene
NGF	Up-regulated gene
NMB	Up-regulated gene
NODAL	Up-regulated gene
NPPA	Up-regulated gene
NRG3	Up-regulated gene
OGN	Down-regulated gene
OSM	Up-regulated gene
PDGFD	Up-regulated gene
PGF	Up-regulated gene
PMCH	Up-regulated gene
PTHLH	Up-regulated gene
REG1A	Up-regulated gene
RETN	Up-regulated gene
SCG2	Up-regulated gene
STC2	Up-regulated gene
TAC1	Down-regulated gene
TDGF1	Down-regulated gene
TNFSF13B	Up-regulated gene
TNFSF14	Up-regulated gene
TNFSF8	Up-regulated gene
TNFSF9	Up-regulated gene
TSLP	Down-regulated gene
UCN	Up-regulated gene
UTS2	Up-regulated gene
VIP	Up-regulated gene
ACVR1C	Down-regulated gene
ADCYAP1R1	Up-regulated gene
ADRB1	Down-regulated gene
ANGPTL1	Down-regulated gene
ANGPTL3	Down-regulated gene
ANGPTL4	Up-regulated gene
APLNR	Up-regulated gene
AVPR1B	Up-regulated gene
AVPR2	Down-regulated gene
BMPR1B	Down-regulated gene
C3AR1	Up-regulated gene
CNTFR	Down-regulated gene
CRLF2	Up-regulated gene
CSF1R	Up-regulated gene
CSF2RA	Up-regulated gene
CSF3R	Up-regulated gene
ESRRB	Down-regulated gene
ESRRG	Down-regulated gene
FLT1	Up-regulated gene
GCGR	Down-regulated gene
HTR3B	Down-regulated gene
HTR3D	Down-regulated gene
IL10RA	Up-regulated gene

Table S4 (*continued*)

Table S4 (*continued*)

Gene	Group
IL12RB1	Up-regulated gene
IL17RE	Down-regulated gene
IL18RAP	Up-regulated gene
IL1RL1	Down-regulated gene
IL20RA	Down-regulated gene
IL20RB	Up-regulated gene
IL21R	Up-regulated gene
IL2RA	Up-regulated gene
IL2RB	Up-regulated gene
IL2RG	Up-regulated gene
IL4R	Up-regulated gene
IL5RA	Down-regulated gene
IL9R	Up-regulated gene
LGR5	Down-regulated gene
MCHR1	Up-regulated gene
MTNR1A	Down-regulated gene
NGFR	Up-regulated gene
NR0B2	Down-regulated gene
NR1I3	Down-regulated gene
NR2E1	Up-regulated gene
NR3C2	Down-regulated gene
NRP2	Up-regulated gene
OPRD1	Up-regulated gene
OSMR	Up-regulated gene
PRLR	Down-regulated gene
PTGER1	Down-regulated gene
PTGER3	Down-regulated gene
PTGFR	Down-regulated gene
PTH1R	Down-regulated gene
RORBw	Down-regulated gene
SORT1	Down-regulated gene
SSTR1	Down-regulated gene
SSTR5	Down-regulated gene
TACR1	Down-regulated gene
TEK	Down-regulated gene
TGFBR3	Down-regulated gene
THRB	Down-regulated gene
TNFRSF14	Up-regulated gene
TNFRSF18	Up-regulated gene
TNFRSF25	Up-regulated gene
TNFRSF4	Up-regulated gene
TNFRSF9	Up-regulated gene
TSHR	Up-regulated gene
TUBB3	Up-regulated gene
ITGAL	Up-regulated gene
ITGB2	Up-regulated gene
TYROBP	Up-regulated gene
LCK	Up-regulated gene
FCGR3A	Up-regulated gene
NCR1	Up-regulated gene
NCR3	Up-regulated gene
CD247	Up-regulated gene
ZAP70	Up-regulated gene
LCP2	Up-regulated gene
LAT	Up-regulated gene
SH3BP2	Up-regulated gene
SHC3	Down-regulated gene
HCST	Up-regulated gene
CD48	Up-regulated gene
CD244	Up-regulated gene
SH2D1A	Up-regulated gene
GZMB	Up-regulated gene
PRF1	Up-regulated gene

Table S4 (*continued*)

http://dx.doi.org/10.21037/tau-20-1348

Table S4 (*continued*)

Gene	Group
CD3D	Up-regulated gene
CD3E	Up-regulated gene
CD3G	Up-regulated gene
PTPRC	Up-regulated gene
ITK	Up-regulated gene
GRAP2	Up-regulated gene
PAK6	Down-regulated gene
PAK7	Down-regulated gene
CD28	Up-regulated gene
ICOS	Up-regulated gene
CTLA4	Up-regulated gene
CBLC	Down-regulated gene
PDK1	Up-regulated gene
PRKCQ	Down-regulated gene

Table S5 Information for 382 differential expression IRGs identified by the univariate Cox regression analysis

Gene	HR (95% CI)	wald.test	P value
CD1D	0.9971 (0.8157-1.219)	0.0000	0.9778
CD4	1.069 (0.901-1.269)	0.5900	0.4431
CD8A	1.058 (0.9723-1.152)	1.7100	0.1905
CD8B	1.046 (0.9626-1.136)	1.1200	0.2896
CD74	1.063 (0.9098-1.242)	0.5900	0.4413
CTSE	0.9472 (0.9094-0.9865)	6.8300	0.0090
CTSS	0.9481 (0.8173-1.1)	0.4900	0.4821
FCER1G	1.282 (1.094-1.503)	9.4100	0.0022
HLA_A	1.169 (0.9329-1.465)	1.8400	0.1748
HLA_B	1.027 (0.8239-1.279)	0.0500	0.8148
HLA_DOB	1.094 (0.9945-1.203)	3.4100	0.0647
HLA_DPA1	0.9017 (0.7874-1.032)	2.2400	0.1343
HLA_DPB1	0.9094 (0.7889-1.048)	1.7200	0.1902
HLA_DQA1	0.9755 (0.8662-1.099)	0.1700	0.6826
HLA_DQA2	0.9543 (0.9014-1.01)	2.5900	0.1074
HLA_DQB1	0.9836 (0.871-1.111)	0.0700	0.7899
HLA_DRA	0.8749 (0.7602-1.007)	3.4800	0.0620
HLA_DRB1	1.051 (0.8985-1.23)	0.3900	0.5318
HLA_F	1.15 (0.9649-1.37)	2.4300	0.1187
HLA_G	0.9173 (0.8472-0.9931)	4.5400	0.0331
HSPA2	1.031 (0.9013-1.18)	0.2000	0.6544
HSPA6	1.27 (1.115-1.447)	13.0000	0.0003
IFNA14	0.9889 (0.9297-1.052)	0.1300	0.7219
IFNG	1.07 (1.006-1.139)	4.6500	0.0311
KIR2DL1	0.9837 (0.9248-1.046)	0.2700	0.6004
KIR2DL3	1.03 (0.9529-1.112)	0.5500	0.4602
KIR2DL4	1.109 (0.9923-1.239)	3.3300	0.0682
KIR3DL1	0.9636 (0.9097-1.021)	1.5900	0.2076
KIR3DL2	0.9799 (0.9302-1.032)	0.5800	0.4456
KLRC1	1.054 (0.9569-1.162)	1.1400	0.2852
KLRC2	1.154 (1.074-1.239)	15.4500	0.0001
KLRD1	1.087 (0.909-1.299)	0.8300	0.3612
LTA	1.165 (1.05-1.293)	8.2600	0.0041
PSMB8	1.099 (0.862-1.4)	0.5800	0.4473
TAP1	1.169 (0.941-1.452)	1.9900	0.1582
TAPBP	1.284 (0.9955-1.656)	3.7100	0.0542
KLRC4	1.031 (0.9864-1.079)	1.8500	0.1742
IFI30	1.409 (1.262-1.574)	36.9600	0.0000
PROCR	1.087 (0.9168-1.29)	0.9300	0.3360
RAET1E	0.7461 (0.6457-0.8622)	15.7700	0.0001
RAET1L	1.012 (0.9797-1.045)	0.5100	0.4754
HAMP	1.253 (1.157-1.357)	30.8400	0.0000
SLPI	1.118 (1.073-1.165)	27.8200	0.0000
CXCL10	1.04 (0.9484-1.141)	0.7000	0.4016
CXCL9	1.038 (0.95-1.134)	0.6800	0.4107
CXCL5	1.088 (1.043-1.135)	15.5100	0.0001
CXCL11	1.056 (0.9667-1.152)	1.4500	0.2283
CXCL13	1.122 (1.059-1.189)	15.1600	0.0001
XCL1	1.189 (1.079-1.31)	12.2100	0.0005
DEFB1	0.9926 (0.9243-1.066)	0.0400	0.8372
TMSB10	1.37 (1.158-1.62)	13.5500	0.0002
LCN2	1.068 (1.02-1.119)	7.7000	0.0055
BPI	1.01 (0.9278-1.101)	0.0600	0.8107
S100A8	1.187 (1.061-1.327)	9.0000	0.0027
PTGDS	1.119 (1.038-1.205)	8.7100	0.0032
PGLYRP2	1.122 (1.07-1.175)	23.2500	0.0000
S100A2	1.105 (1.007-1.213)	4.4700	0.0345
DEFB125	1.037 (0.9972-1.079)	3.3200	0.0686
DEFB132	0.9991 (0.9523-1.048)	0.0000	0.9715
S100A5	1.046 (0.9721-1.125)	1.4400	0.2295
TMSB4Y	0.9835 (0.9579-1.01)	1.5400	0.2147
TMSB15B	1.016 (0.9259-1.116)	0.1200	0.7337
S100Z	1.062 (0.9645-1.17)	1.5000	0.2202
S100A14	1.016 (0.9198-1.122)	0.1000	0.7556
AZU1	1.048 (0.9871-1.112)	2.3500	0.1254
WFDC2	1.053 (0.9824-1.13)	2.1400	0.1437
UMODL1	1.054 (1.008-1.102)	5.2800	0.0216
TGFB1	1.438 (1.167-1.772)	11.6400	0.0006
MMP9	1.149 (1.072-1.231)	15.3600	0.0001
APOBEC3G	1.322 (1.131-1.546)	12.2500	0.0005
FABP6	1.065 (0.9862-1.15)	2.5800	0.1083
NOD2	1.356 (1.191-1.545)	21.0200	0.0000
MBL2	1.066 (1.033-1.099)	16.3600	0.0001
TLR2	1.27 (1.071-1.506)	7.5300	0.0061
PLAU	1.351 (1.194-1.53)	22.5700	0.0000
PAEP	1.082 (1.053-1.111)	32.9900	0.0000
LPA	0.95 (0.9136-0.9879)	6.6100	0.0101
RBP4	0.9866 (0.9456-1.029)	0.3900	0.5349
LTF	0.9249 (0.868-0.9855)	5.8100	0.0159
FABP7	1.013 (0.975-1.054)	0.4600	0.4980
FABP5	1.405 (1.211-1.63)	20.1700	0.0000
OASL	1.333 (1.168-1.521)	18.1800	0.0000
CRABP2	1.185 (1.117-1.257)	31.5800	0.0000
CRABP1	1.026 (1-1.053)	3.8500	0.0497
RBP2	1.008 (0.9633-1.055)	0.1200	0.7311
PMP2	0.9925 (0.9595-1.027)	0.1900	0.6604
APOD	1.073 (0.9788-1.176)	2.2600	0.1327
PRTN3	1.037 (0.9991-1.077)	3.6500	0.0560
CYBB	0.9601 (0.8561-1.077)	0.4800	0.4866
ISG20	1.458 (1.24-1.714)	20.8200	0.0000
DUOX2	1.056 (0.9897-1.126)	2.7100	0.0997
IDO1	0.9996 (0.9032-1.106)	0.0000	0.9941
SEMG1	1.037 (0.9892-1.088)	2.2900	0.1304
CCL20	1.048 (0.9856-1.114)	2.2400	0.1348
CHIT1	0.9889 (0.9411-1.039)	0.1900	0.6590
CD40	1.149 (0.9054-1.457)	1.3000	0.2538
TLR7	0.9289 (0.8339-1.035)	1.7900	0.1804
VEGFA	1.011 (0.8859-1.154)	0.0300	0.8690
ISG15	1.369 (1.209-1.55)	24.6000	0.0000
TFR2	1.134 (1.059-1.213)	13.1400	0.0003
IL27	1.169 (1.059-1.291)	9.5400	0.0020
LYZ	0.8992 (0.8193-0.987)	4.9900	0.0254
CCL5	1.167 (1.05-1.298)	8.2100	0.0042
CCR6	0.9746 (0.919-1.034)	0.7400	0.3912
TLR8	0.955 (0.8607-1.06)	0.7500	0.3857
GNLY	1.144 (1.009-1.297)	4.4100	0.0358
PDGFRA	1.064 (0.9945-1.139)	3.2500	0.0716

Table S5 (*continued*)

Table S5 (*continued*)

http://dx.doi.org/10.21037/tau-20-1348

Table S5 (*continued*)

Gene	HR (95% CI)	wald.test	P value
MSR1	0.9744 (0.8573-1.107)	0.1600	0.6910
DLL4	0.8588 (0.7543-0.9779)	5.2800	0.0216
SLC11A1	1.441 (1.273-1.632)	33.1900	0.0000
SEMG2	1.013 (0.9633-1.065)	0.2600	0.6130
DES	1.013 (0.9651-1.063)	0.2600	0.6077
TNFRS-F10B	1.597 (1.247-2.045)	13.8000	0.0002
CCL4	1.138 (1.01-1.282)	4.5300	0.0333
APOBEC3H	1.285 (1.13-1.46)	14.7500	0.0001
TMPRSS6	1.161 (1.081-1.247)	16.7200	0.0000
MARCO	1.132 (1.052-1.219)	10.9200	0.0010
KNG1	1.018 (0.9809-1.056)	0.8600	0.3527
KLRK1	1.181 (1.083-1.287)	14.2300	0.0002
RNASE3	1.018 (0.9649-1.075)	0.4400	0.5094
IRF7	1.536 (1.308-1.805)	27.2600	0.0000
LTB4R	1.565 (1.355-1.807)	37.2900	0.0000
IL7R	0.9419 (0.8466-1.048)	1.2100	0.2718
APOBEC3C	1.288 (1.093-1.517)	9.1800	0.0024
PTGS2	1.105 (1.015-1.203)	5.3100	0.0212
CD40LG	1.009 (0.9136-1.114)	0.0300	0.8643
CD14	1.275 (1.094-1.486)	9.6500	0.0019
MASP1	0.8723 (0.8134-0.9355)	14.6500	0.0001
PROC	0.986 (0.9111-1.067)	0.1200	0.7258
HRG	0.9921 (0.9575-1.028)	0.1900	0.6625
HMOX1	0.9387 (0.8316-1.06)	1.0500	0.3064
STAB2	1.115 (1.014-1.226)	5.0100	0.0252
PDCD1	1.119 (1.033-1.212)	7.6800	0.0056
PCSK2	1.038 (0.9959-1.082)	3.1100	0.0777
ARG2	1.071 (0.9916-1.157)	3.0400	0.0810
AQP9	1.139 (1.066-1.216)	14.9300	0.0001
FASLG	1.113 (1.011-1.224)	4.8100	0.0283
APOH	1.058 (1.012-1.106)	6.3000	0.0121
BIRC5	1.494 (1.325-1.684)	43.1700	0.0000
VIM	1.3 (1.057-1.598)	6.1700	0.0130
VCAM1	0.9496 (0.868-1.039)	1.2700	0.2590
GBP2	1.351 (1.13-1.615)	10.8900	0.0010
ALB	0.973 (0.905-1.046)	0.5500	0.4576
OAS1	1.105 (0.9057-1.347)	0.9600	0.3263
AGER	1.368 (1.209-1.549)	24.6500	0.0000
NOS1	0.9321 (0.8707-0.9979)	4.0900	0.0432
CCL18	1.016 (0.9645-1.07)	0.3600	0.5501
CCL22	0.9097 (0.8467-0.9775)	6.6700	0.0098
CCR7	1.035 (0.9234-1.161)	0.3600	0.5510
CCR8	1.05 (0.9962-1.107)	3.3100	0.0689
CCL21	1.027 (0.9862-1.07)	1.6600	0.1978
CCL3	1.109 (0.9979-1.233)	3.6900	0.0546
CCL11	1.066 (1.028-1.105)	12.0900	0.0005
CCR5	1.052 (0.9467-1.168)	0.8800	0.3482
CCL3L3	0.9856 (0.9314-1.043)	0.2500	0.6145
CCL4L1	1.03 (0.9521-1.114)	0.5400	0.4627
XCL2	1.187 (1.069-1.317)	10.3300	0.0013
CXCR4	1.182 (0.9943-1.406)	3.5900	0.0581
CXCR6	1.072 (0.9571-1.202)	1.4500	0.2287
FAM19A4	1.024 (0.9874-1.061)	1.6200	0.2027
FAM19A1	0.9818 (0.9046-1.065)	0.1900	0.6592
CDH1	0.7951 (0.7161-0.8827)	18.4600	0.0000
IL10	1.115 (1.01-1.231)	4.6300	0.0314
CRP	1.063 (1.022-1.105)	9.2900	0.0023
PTGDR	1.172 (1.024-1.342)	5.2800	0.0216
CD86	1.109 (0.9534-1.29)	1.8000	0.1798
HCK	1.135 (0.9504-1.356)	1.9600	0.1619
VDR	0.9412 (0.8169-1.084)	0.7000	0.4015
OLR1	1.039 (0.9317-1.159)	0.4700	0.4919

Table S5 (*continued*)

Table S5 (*continued*)

Gene	HR (95% CI)	wald.test	P value
RNASE2	1.303 (1.165-1.458)	21.4700	0.0000
CD79A	1.084 (1.004-1.171)	4.2200	0.0399
BTK	1.077 (0.9096-1.276)	0.7500	0.3878
VAV1	1.159 (0.992-1.354)	3.4500	0.0631
RAC2	1.221 (1.06-1.407)	7.6200	0.0058
CHP2	1.035 (0.9974-1.073)	3.3100	0.0688
CARD11	1.193 (1.074-1.325)	10.8700	0.0010
CR2	1.003 (0.9574-1.051)	0.0200	0.8983
PIK3R5	1.105 (0.9392-1.301)	1.4500	0.2279
INPP5D	1.073 (0.8746-1.316)	0.4600	0.4993
CD72	1.334 (1.174-1.516)	19.5200	0.0000
LILRB3	1.47 (1.268-1.704)	26.0200	0.0000
FCGR2B	1.183 (1.048-1.335)	7.3600	0.0067
C3	1.119 (1.014-1.234)	4.9800	0.0257
EDN1	0.8403 (0.7657-0.9222)	13.4500	0.0002
EDN3	1.001 (0.9693-1.034)	0.0000	0.9522
FGF10	1.023 (0.9894-1.057)	1.7700	0.1836
SEMA3B	1.117 (0.9971-1.252)	3.6500	0.0562
SEMA3D	0.8914 (0.8435-0.9421)	16.6300	0.0000
SEMA3E	1.108 (1.065-1.152)	25.8800	0.0000
SEMA3G	0.7207 (0.6552-0.7928)	45.3200	0.0000
SEMA5B	0.8932 (0.8186-0.9745)	6.4500	0.0111
SEMA6A	0.8171 (0.7262-0.9194)	11.2600	0.0008
SEMA6B	1.01 (0.8602-1.187)	0.0200	0.9002
SEMA6D	0.761 (0.6714-0.8624)	18.2900	0.0000
SLIT2	0.977 (0.8853-1.078)	0.2100	0.6436
TYMP	1.434 (1.21-1.698)	17.3600	0.0000
CCR9	1.007 (0.9525-1.065)	0.0600	0.8029
CX3CR1	0.8638 (0.7857-0.9496)	9.1700	0.0025
CXCR3	1.094 (0.9975-1.2)	3.6400	0.0565
FPR1	1.026 (0.9119-1.155)	0.1800	0.6690
LTB4R2	1.367 (1.177-1.587)	16.7900	0.0000
PLAUR	1.595 (1.394-1.824)	46.4200	0.0000
PLXNA4	1.124 (1.03-1.228)	6.8200	0.0090
PLXNB3	1.393 (1.275-1.521)	54.1500	0.0000
PLXNC1	0.999 (0.8576-1.164)	0.0000	0.9896
PLXND1	0.9333 (0.7795-1.118)	0.5600	0.4530
XCR1	0.9281 (0.8686-0.9916)	4.8800	0.0271
ADM	0.9923 (0.8511-1.157)	0.0100	0.9218
ADM2	0.9231 (0.8272-1.03)	2.0500	0.1526
AGRP	1.09 (1.023-1.162)	7.0600	0.0079
AMH	1.217 (1.123-1.319)	22.8000	0.0000
ANGPTL7	1.022 (0.9868-1.058)	1.4700	0.2249
APLN	0.879 (0.7726-1)	3.8400	0.0502
BDNF	0.9225 (0.8517-0.9992)	3.9200	0.0478
BMP1	1.725 (1.432-2.078)	32.8800	0.0000
BMP3	0.9922 (0.9338-1.054)	0.0600	0.8013
BMP5	0.9738 (0.9435-1.005)	2.7100	0.1000
BMP6	0.8032 (0.7107-0.9078)	12.3100	0.0004
BMP7	1.055 (1.009-1.103)	5.6300	0.0177
BTC	0.9373 (0.8399-1.046)	1.3400	0.2475
CALCA	0.9827 (0.9524-1.014)	1.2000	0.2741
CD70	1.034 (0.9736-1.099)	1.1900	0.2746
CGA	1.046 (1.014-1.079)	8.2300	0.0041
CGB7	1.094 (1.02-1.173)	6.3900	0.0115
CHGA	1.116 (1.06-1.174)	17.5700	0.0000
CHGB	1.054 (0.9852-1.127)	2.3300	0.1273
CMTM3	1.528 (1.28-1.825)	22.0200	0.0000
CMTM4	0.765 (0.6403-0.9141)	8.7000	0.0032
EBI3	1.26 (1.089-1.458)	9.6600	0.0019
EGF	0.9896 (0.922-1.062)	0.0800	0.7726
EPGN	1.036 (0.9994-1.075)	3.7100	0.0541
EPO	1.04 (1.006-1.075)	5.2100	0.0224

Table S5 (*continued*)

http://dx.doi.org/10.21037/tau-20-1348

Table S5 (*continued*)

Gene	HR (95% CI)	wald.test	P value
ESM1	0.8378 (0.7597-0.924)	12.5400	0.0004
FAM3B	1.028 (0.9625-1.097)	0.6700	0.4147
FGF1	0.836 (0.7459-0.9369)	9.4900	0.0021
FGF20	0.9713 (0.9247-1.02)	1.3500	0.2445
FGF7	1.056 (0.9968-1.12)	3.4300	0.0641
FGF9	0.9887 (0.9531-1.026)	0.3700	0.5451
GDF6	0.861 (0.8067-0.919)	20.2900	0.0000
GDF7	0.8155 (0.7323-0.9082)	13.7900	0.0002
GDNF	1.001 (0.9552-1.048)	0.0000	0.9772
GMFG	1.078 (0.8791-1.323)	0.5200	0.4689
GNRH1	1.377 (1.228-1.545)	29.7800	0.0000
GREM1	1.103 (1.045-1.164)	12.5900	0.0004
GREM2	1.092 (1.043-1.143)	14.1800	0.0002
IGF2	1.012 (0.9508-1.078)	0.1500	0.7003
IL11	1.114 (1.046-1.187)	11.4000	0.0007
IL16	1.002 (0.8434-1.191)	0.0000	0.9806
IL19	1.023 (0.9869-1.061)	1.5600	0.2121
IL24	1.047 (0.8792-1.248)	0.2700	0.6041
IL32	1.111 (0.9661-1.277)	2.1800	0.1399
INHBB	0.9928 (0.8858-1.113)	0.0200	0.9011
INHBE	1.201 (1.122-1.286)	27.6300	0.0000
JAG2	0.825 (0.7039-0.967)	5.6400	0.0176
KITLG	0.7393 (0.6415-0.852)	17.4000	0.0000
KL	0.7686 (0.7125-0.8291)	46.3800	0.0000
LEFTY2	0.9685 (0.929-1.01)	2.2700	0.1318
NGF	1.095 (0.9721-1.233)	2.2300	0.1355
NMB	1.117 (0.9988-1.249)	3.7600	0.0526
NODAL	1.053 (0.9628-1.153)	1.2900	0.2566
NPPA	1.053 (0.9937-1.116)	3.0400	0.0810
NRG3	0.8713 (0.7647-0.9928)	4.2800	0.0386
OGN	0.9907 (0.9436-1.04)	0.1400	0.7069
OSM	1.259 (1.14-1.39)	20.7800	0.0000
PDGFD	0.6796 (0.6102-0.7569)	49.3700	0.0000
PGF	1.108 (1.022-1.202)	6.1500	0.0131
PMCH	1.047 (1.006-1.089)	5.1800	0.0229
PTHLH	1.077 (1.018-1.139)	6.7500	0.0094
REG1A	0.9924 (0.9559-1.03)	0.1600	0.6922
RETN	1.052 (0.9894-1.118)	2.6100	0.1060
SCG2	1.094 (1.019-1.175)	6.0900	0.0136
STC2	1.024 (0.9065-1.156)	0.1400	0.7065
TAC1	0.9849 (0.9565-1.014)	1.0300	0.3090
TDGF1	1.008 (0.9616-1.057)	0.1100	0.7418
TNFSF13B	1.292 (1.138-1.466)	15.6700	0.0001
TNFSF14	1.294 (1.185-1.413)	32.9000	0.0000
TNFSF8	0.9021 (0.7918-1.028)	2.3900	0.1218
TNFSF9	1.109 (0.9986-1.232)	3.7400	0.0532
TSLP	1.117 (1.015-1.23)	5.0900	0.0240
UCN	1.502 (1.325-1.703)	40.4400	0.0000
UTS2	1.047 (0.9885-1.109)	2.4600	0.1171
VIP	1.024 (0.9599-1.092)	0.5100	0.4730
ACVR1C	1.085 (1.005-1.171)	4.3600	0.0368
ADCY-AP1R1	1.004 (0.9345-1.079)	0.0100	0.9117
ADRB1	1.054 (0.9778-1.136)	1.8900	0.1693
ANGPTL1	0.9619 (0.8979-1.031)	1.2200	0.2700
ANGPTL3	0.8716 (0.8205-0.926)	19.8300	0.0000
ANGPTL4	0.9857 (0.9072-1.071)	0.1200	0.7342
APLNR	0.7734 (0.7022-0.8517)	27.2300	0.0000
AVPR1B	0.9374 (0.9036-0.9726)	11.8300	0.0006
AVPR2	0.9477 (0.8718-1.03)	1.5900	0.2080
BMPR1B	1.045 (0.9961-1.096)	3.2400	0.0721
C3AR1	0.9389 (0.814-1.083)	0.7500	0.3871
CNTFR	1.013 (0.9675-1.06)	0.2900	0.5885

Table S5 (*continued*)

Table S5 (*continued*)

Gene	HR (95% CI)	wald.test	P value
CRLF2	1.053 (0.9409-1.178)	0.8000	0.3705
CSF1R	1.095 (0.937-1.279)	1.3000	0.2544
CSF2RA	1.099 (0.8103-1.491)	0.3700	0.5433
CSF3R	1.282 (1.111-1.48)	11.5200	0.0007
ESRRB	1.013 (0.9272-1.108)	0.0900	0.7685
ESRRG	0.832 (0.7781-0.8897)	28.9000	0.0000
FLT1	0.7624 (0.687-0.8461)	26.0700	0.0000
GCGR	1.027 (0.9957-1.058)	2.8300	0.0923
HTR3B	0.9995 (0.9623-1.038)	0.0000	0.9794
HTR3D	1.036 (0.9991-1.075)	3.6500	0.0562
IL10RA	1.183 (1.023-1.367)	5.1500	0.0233
IL12RB1	1.139 (0.9847-1.318)	3.0700	0.0797
IL17RE	1.003 (0.8672-1.161)	0.0000	0.9645
IL18RAP	1.1 (0.9673-1.252)	2.1200	0.1457
IL1RL1	0.9127 (0.8575-0.9715)	8.2300	0.0041
IL20RA	1.099 (1.05-1.149)	16.6600	0.0000
IL20RB	1.174 (1.116-1.234)	39.0600	0.0000
IL21R	1.228 (1.078-1.397)	9.6200	0.0019
IL2RA	1.2 (1.088-1.324)	13.1900	0.0003
IL2RB	1.16 (1.01-1.331)	4.4300	0.0354
IL2RG	1.172 (1.037-1.324)	6.4800	0.0109
IL4R	1.627 (1.215-2.179)	10.6600	0.0011
IL5RA	1.039 (0.9607-1.125)	0.9300	0.3357
IL9R	1.112 (0.9341-1.324)	1.4300	0.2325
LGR5	1.011 (0.9658-1.057)	0.2100	0.6502
MCHR1	1.042 (0.9938-1.092)	2.8900	0.0892
MTNR1A	1.005 (0.9753-1.036)	0.1100	0.7435
NGFR	0.873 (0.7869-0.9686)	6.5600	0.0104
NR0B2	0.995 (0.9687-1.022)	0.1300	0.7135
NR1I3	0.9488 (0.7917-1.137)	0.3200	0.5695
NR2E1	1.027 (0.9912-1.065)	2.1900	0.1388
NR3C2	0.684 (0.6156-0.7599)	49.9500	0.0000
NRP2	1.027 (0.8705-1.211)	0.1000	0.7533
OPRD1	1.283 (1.157-1.422)	22.2900	0.0000
OSMR	1.204 (1.007-1.44)	4.1700	0.0412
PRLR	0.9223 (0.8392-1.014)	2.8200	0.0930
PTGER1	1.113 (1.066-1.161)	23.6800	0.0000
PTGER3	0.883 (0.8272-0.9426)	13.9500	0.0002
PTGFR	1.033 (0.9575-1.115)	0.7100	0.4005
PTH1R	0.8624 (0.7901-0.9412)	11.0100	0.0009
RORB	1.102 (1.038-1.171)	10.0700	0.0015
SORT1	0.7218 (0.5917-0.8804)	10.3500	0.0013
SSTR1	0.8821 (0.8332-0.9339)	18.5900	0.0000
SSTR5	1.009 (0.9786-1.04)	0.3200	0.5718
TACR1	0.8905 (0.8405-0.9435)	15.4500	0.0001
TEK	0.661 (0.5963-0.7327)	62.0800	0.0000
TGFBR3	0.6589 (0.5533-0.7845)	21.9500	0.0000
THRB	0.7559 (0.6809-0.8391)	27.5800	0.0000
TNFRSF14	1.096 (0.9182-1.308)	1.0300	0.3099
TNFRSF18	1.343 (1.201-1.502)	26.6000	0.0000
TNFRSF25	1.291 (1.146-1.455)	17.5600	0.0000
TNFRSF4	1.145 (0.9977-1.315)	3.7100	0.0539
TNFRSF9	1.1 (1.019-1.188)	5.9300	0.0149
TSHR	1.012 (0.9206-1.113)	0.0600	0.8014
TUBB3	1.253 (1.161-1.352)	33.4700	0.0000
ITGAL	1.099 (0.9618-1.256)	1.9300	0.1651
ITGB2	1.076 (0.9246-1.251)	0.8900	0.3446
TYROBP	1.17 (1.004-1.364)	4.0300	0.0446
LCK	1.071 (0.9487-1.21)	1.2400	0.2664
FCGR3A	1.169 (1.024-1.335)	5.3500	0.0208
NCR1	1.004 (0.9128-1.105)	0.0100	0.9298
NCR3	1.03 (0.8956-1.185)	0.1700	0.6760
CD247	1.082 (0.9421-1.243)	1.2500	0.2639

Table S5 (*continued*)

http://dx.doi.org/10.21037/tau-20-1348

Table S5 (*continued*)

Gene	HR (95% CI)	wald.test	P value
ZAP70	1.263 (1.114-1.432)	13.2500	0.0003
LCP2	1.136 (0.9377-1.377)	1.7000	0.1922
LAT	1.219 (1.113-1.334)	18.3100	0.0000
SH3BP2	0.9829 (0.8002-1.207)	0.0300	0.8697
SHC3	1.21 (1.068-1.371)	8.9100	0.0028
HCST	1.333 (1.176-1.511)	20.2800	0.0000
CD48	1.02 (0.8893-1.169)	0.0800	0.7791
CD244	1.092 (0.9463-1.26)	1.4500	0.2288
SH2D1A	1.068 (0.9617-1.186)	1.5100	0.2192
GZMB	1.191 (1.046-1.355)	6.9900	0.0082
PRF1	1.01 (0.8847-1.154)	0.0200	0.8780
CD3D	1.076 (0.9746-1.189)	2.1100	0.1465
CD3E	1.087 (0.9787-1.208)	2.4300	0.1190
CD3G	1.007 (0.9079-1.118)	0.0200	0.8911
PTPRC	0.9737 (0.8521-1.113)	0.1500	0.6953
ITK	1.059 (0.9375-1.197)	0.8500	0.3552
GRAP2	1.012 (0.8767-1.169)	0.0300	0.8663
PAK6	1.052 (1.009-1.097)	5.6000	0.0180
PAK7	1.039 (1.004-1.074)	4.9000	0.0269
CD28	1.089 (0.9705-1.221)	2.1000	0.1474
ICOS	1.059 (0.9668-1.161)	1.5300	0.2167
CTLA4	1.175 (1.073-1.286)	12.2000	0.0005
CBLC	1.01 (0.9406-1.085)	0.0800	0.7763
PDK1	0.8721 (0.7111-1.07)	1.7300	0.1887
PRKCQ	0.878 (0.7667-1.006)	3.5400	0.0601

http://dx.doi.org/10.21037/tau-20-1348

Table S6 Information for 8 candidate IRGs identified by the multivariate Cox regression analysis

Gene	HR	95% CI	coef	P value
CRABP2	1.07676	1.0011-1.1582	0.07396	0.04669
LTB4R	1.17957	1.0013-1.3895	0.16515	0.04817
PLAUR	1.15893	0.9737-1.3794	0.1475	0.09689
PLXNB3	1.07077	0.9532-1.2028	0.06838	0.24901
KL	1.01536	0.9014-1.1437	0.01525	0.80181
IL20RB	1.05249	0.9898-1.1191	0.05115	0.10246
PTGER1	1.05377	1.0075-1.1022	0.05238	0.02223
TEK	0.81594	0.7110-0.9363	-0.20342	0.00377

Table S7 immune cell infiltration in two groups

Immune cell type	Low-risk group	High-risk group
B cell naive_CIBERSORT	0.0157494	0.0101317
B cell memory_CIBERSORT	0.00053044	0.002702
B cell plasma_CIBERSORT	0.05507898	0.0458001
T cell CD8+_CIBERSORT	0.15163708	0.1820687
T cell CD4+ naive_CIBERSORT	0	3.689E-05
T cell CD4+ memory resting_CIBERSORT	0.14163721	0.1243761
T cell CD4+ memory activated_CIBERSORT	0.00030018	0.0021332
T cell follicular helper_CIBERSORT	0.02126128	0.0350954
T cell regulatory (Tregs)_CIBERSORT	0.00902234	0.0205732
T cell gamma delta_CIBERSORT	0.0216898	0.0204485
NK cell resting_CIBERSORT	0.00976917	0.0090843
NK cell activated_CIBERSORT	0.04972058	0.0598868
Monocyte_CIBERSORT	0.05737104	0.0467553
Macrophage M0_CIBERSORT	0.00726102	0.0274406
Macrophage M1_CIBERSORT	0.0631331	0.0547069
Macrophage M2_CIBERSORT	0.34385585	0.3146842
Myeloid dendritic cell resting_CIBERSORT	0.00323255	0.0012643
Myeloid dendritic cell activated_CIBERSORT	0.00204996	0.0016187
Mast cell activated_CIBERSORT	0.02880841	0.0189666
Mast cell resting_CIBERSORT	0.01334313	0.0156609
Eosinophil_CIBERSORT	0.00025604	0.0001598
Neutrophil_CIBERSORT	0.00429245	0.0064058

http://dx.doi.org/10.21037/tau-20-1348

Table S8 Clinical information of patients

Variable	No. of patients
Gender	
Male	23
Female	12
Age	
≥60	9
<60	26
Histological grade	
G1	7
G2	23
G3	2
G4	3
Stage	
I	18
II	5
III	6
IV	6
T stage	
I	21
II	7
III	7
IV	0
N stage	
N0	33
N1	2
M stage	
M0	31
M1	4

Table S9 Variable corresponding point

Variable	Point
Age	
≥60	7
<60	0
Gender	
Male	0
Female	1
T stage	
I	1
II	0
III	5
IV	6
N stage	
N0	3
N1	5
Nx	0
M stage	
M0	20
M1	36
Mx	0
Histological grade	
G1	0
G2	94
G3	97
G4	100
Necrosis	
Yes	9
No	0
Risk_score	
–1	0
–0.5	9
0	18
0.5	26
1	35
1.5	44
2	53
2.5	62
3	70

http://dx.doi.org/10.21037/tau-20-1348